

Higgs-boson signals in superstring-inspired models at hadron supercolliders

Howard Baer

High Energy Physics Division, Argonne National Laboratory, Argonne, Illinois 60439

Duane Dicus

Center for Particle Theory, Physics Department, University of Texas, Austin, Texas 78712

Manuel Drees and Xerxes Tata

Physics Department, University of Wisconsin, Madison, Wisconsin 53706

(Received 6 March 1987)

In superstring-inspired E_6 supergravity models, the mass of the lightest Higgs scalar (H_L) is expected to be below ~ 170 GeV if E_6 is broken directly to a rank-5 subgroup and below ~ 210 GeV if intermediate scales of $\sim 10^{10}$ GeV are allowed. We show that if the mass of the additional neutral gauge boson $Z^{0'}$ is less than about 600 GeV, then $\sim 10^4$ – 10^5 $Z^{0'} \rightarrow Z^0 H_L$ pairs may be expected per 10^4 pb $^{-1}$, the annual integrated luminosity anticipated at the proposed 40-TeV pp supercollider. This large rate allows us to use the clean $Z^0 \rightarrow l\bar{l}$ decays as a trigger for the Higgs-boson search. We find that even if $H_L \rightarrow t\bar{t}$ decays dominate, a signal-to-background ratio substantially exceeding unity is expected for reasonable experimental resolutions on the measurement of $Z^0 t\bar{t}$ and $t\bar{t}$ invariant masses. We further show that for a wide range of parameters, H_L can decay into chargino and neutralino pairs. These decays lead to hadron-free $Z^0 + \text{missing } p_T$ (\cancel{p}_T) events which may stand out over the $Z^0 Z^0$ background and also to spectacular $Z^0 + n$ lepton + \cancel{p}_T events ($n \leq 4$) which are almost free of standard-model backgrounds.

I. INTRODUCTION

The discovery¹ of anomaly-free superstring theories has provided a tremendous impetus for the study of the low-energy effective field theory^{2–7} resulting from the compactification from ten to four dimensions. This is generally believed to be a supergravity theory based on the gauge group E_6 , with all the chiral superfields transforming as the 27 or 27* representation of the gauge group.^{2,3} E_6 is broken by the Hosotani mechanism⁸ to the low-energy gauge group, which has rank ≥ 5 (Refs. 2 and 3). These models, therefore, contain at least one extra neutral gauge boson $Z^{0'}$ which may be relatively light.

The extra $Z^{0'}$ boson(s) may be searched for in the CERN collider data. Absence of their signals implies that $M_{Z^{0'}} > 105$ – 140 GeV depending on the mass of exotic fermions in the model.⁵ From the analysis of the effective number of light-neutrino species that can be accommodated without spoiling the successful predictions of nucleosynthesis for the abundance of light elements, it has been claimed that $M_{Z^{0'}} \gtrsim 400$ GeV (Ref. 9) for the rank-5 model of Ref. 6. If a larger number of neutrino species can be accommodated by the data, as suggested in Ref. 10, considerably smaller ($M_{Z^{0'}} \gtrsim 300$ GeV) values of $Z^{0'}$ mass are allowed.

The existence of an extra boson opens up the possibility that the cross section for the production of other new particles may be resonance enhanced. In particular, it has been suggested¹¹ that it may be possible to search for the Higgs boson produced via the decay $Z^{0'} \rightarrow Z^0 + H$. Apart from the fact that the cross section is greatly

enhanced, the leptonic decay of $Z^{0'}$ can serve as a trigger for the Higgs-boson search.

The Higgs sector of the low-energy theory is quite complicated. Although no upper bounds on the mass of the lightest scalar can be derived from just the structure of the low-energy potential, fairly restrictive bounds can be obtained if some general assumptions are made. For instance, if we assume that there is no new physics intervening between the weak scale and the grand-unification scale, the requirement that all couplings remain perturbative implies that there be a scalar with mass $\lesssim 170$ GeV in all models with $SU(3) \times SU(2) \times U(1) \times \tilde{U}(1)$ as the low-energy gauge group.¹² If we further require that supersymmetry (SUSY) breaking effectively occurs only due to gaugino masses, the bound is strengthened to 110 GeV (Ref. 12). In models with an intermediate scale $M_I \sim 10^{10}$ GeV, the weaker requirement that the Higgs-boson coupling remain perturbative in the range from M_W to M_I translates to a bound of 210 GeV (Ref. 12). We thus see that for a wide class of models, the decay $Z^{0'} \rightarrow Z^0 + H_L$ (H_L is the lightest Higgs boson) is likely to be possible unless it is suppressed by small couplings. This coupling arises from the two-gauge-boson–two-Higgs-boson vertex where one of the Higgs fields is set equal to its vacuum expectation value. It is thus of the form gauge coupling $\times M_Z \times$ a factor depending on the $\tilde{U}(1)$ charges and Higgs-boson mixing angles plus small corrections due to Z^0 - $Z^{0'}$ mixing. We find a nonvanishing value of this coupling independent of $M_{Z^{0'}}$ even when the Z^0 - $Z^{0'}$ mixing is zero.^{11,13}

The purpose of this paper is to explore the possibility of discovering the Higgs boson by studying the decay of

Z^0 at a multi-TeV hadron collider using the associated Z^0 as a trigger for the Higgs-boson signal. The cross section for $pp \rightarrow Z^0 X \rightarrow Z^0 H_L X$ is sensitive to the masses and mixing angles of the model. For the rank-5 model⁶ the $Z^0 H_L$ cross section at $\sqrt{s}=40$ TeV varies between 1 and 25 pb for $M_{Z^0}=400$ GeV and is typically ten times smaller for $M_{Z^0}=800$ GeV. This corresponds to an annual rate of $\sim 10^4 - 10^5$ $Z^0 H_L$ pairs at the proposed Superconducting Super Collider (SSC), assuming an integrated luminosity of 10^4 pb⁻¹ per year.

As we have already discussed, it is rather unlikely that the decays $H_L \rightarrow W^+ W^-$ or $Z^0 Z^0$ will be kinematically accessible. Unless the top quark is very heavy, the dominant Higgs-boson decay is $H_L \rightarrow t\bar{t}$. This gives rise to $t\bar{t}$ pairs in association with Z^0 with $M_{t\bar{t}}=m_H$ and $M_{Z^0 t\bar{t}}=M_{Z^0}$. The dominant background, which comes from $gg \rightarrow Z^0 t\bar{t}$ has been estimated by Gunion and Kunzst.¹⁴ We will see that, with reasonable values of resolution for $M_{Z^0 t\bar{t}}$ and $M_{t\bar{t}}$, the signal exceeds the background, provided the top quark can be identified with reasonable efficiency.

In the class of models we are considering, for $M_{Z^0} \sim 0.5$ TeV, there is a large range of parameters for which the light chargino (\tilde{W}) and the two lighter neutralinos (\tilde{Z}_1, \tilde{Z}_2) have mass $\lesssim 50$ GeV so that the decays

$$H_L \rightarrow \tilde{W} \tilde{W}^*, \quad (1.1)$$

$$H_L \rightarrow \tilde{Z}_1 \tilde{Z}_1, \tilde{Z}_1 \tilde{Z}_2 \text{ and } \tilde{Z}_2 \tilde{Z}_2, \quad (1.2)$$

have substantial branching fractions. If \tilde{Z}_1 is indeed the lightest supersymmetric particle, as is expected in many models, it will escape detection. Thus an event with $Z^0 \rightarrow Z^0 H_L \rightarrow Z^0 + \tilde{Z}_1 \tilde{Z}_1$ will contain a Z^0 with large p_T recoiling against nothing with the p_T having a Jacobian peak characteristic of the two-body decay of the Z^0 .

Since we require the Z^0 produced via $Z^0 \rightarrow Z^0 + H_L$ to decay leptonically, the main standard-model background comes from Z^0 pair production with one of the Z^0 's decaying via $Z^0 \rightarrow \nu\bar{\nu}$. We do not consider the possibility of triggering on hadronic decays of Z^0 since these have large QCD backgrounds.¹⁵

Finally, we come to signals resulting from $H_L \rightarrow \tilde{W} \tilde{W}^*, \tilde{Z}_1 \tilde{Z}_2$, and $\tilde{Z}_2 \tilde{Z}_2$. If the \tilde{W} and \tilde{Z}_2 decay leptonically this gives rise to characteristic multilepton events free from hadronic activity. It is further argued (see Sec. III) that in the class of models where SUSY breaking is dominantly due to gaugino masses, the hadronic decays of \tilde{Z}_2 are strongly suppressed so that \tilde{Z}_2 almost exclusively decays via

$$\tilde{Z}_2 \rightarrow \tilde{Z}_1 \bar{l} \quad (1.3a)$$

or

$$\tilde{Z}_2 \rightarrow \tilde{Z}_1 \nu \bar{\nu}. \quad (1.3b)$$

The decays (1.3a) lead to multilepton signals, whereas decays (1.3b) add to the $Z^0 +$ missing p_T (\cancel{p}_T) signal discussed for $H_L \rightarrow \tilde{Z}_1 \tilde{Z}_1$ decay.

The rest of this paper is organized as follows. In Sec. II we study the $Z^0 Z^0 H_L$ vertex and present our results for the cross section for $pp \rightarrow Z^0 X \rightarrow Z^0 H_L X$ that may be expected at a 40-TeV pp collider. The branching fractions for the various decays of the Higgs boson are studied in Sec. III. The discussion presented here is quite general and so is also applicable for studying supersymmetric Higgs-particle signatures when the Higgs particle is produced by other processes. The decays of \tilde{W} and \tilde{Z}_2 are discussed in Sec. IV. The rates for the various signals resulting from $Z^0 \rightarrow Z^0 H_L$ at the SSC and the corresponding backgrounds are discussed in Sec. V. We conclude in Sec. VI with some general remarks and a summary of our results.

II. HIGGS-BOSON PRODUCTION VIA Z^0 DECAYS

The low-energy superpotential for superstring-motivated models is purely cubic and the breaking of electroweak symmetry is achieved by the introduction of a field N that is a singlet under $SU(3)_C \times SU(2)_L \times U(1)_Y$ but transforms nontrivially under the additional gauge group.²⁻⁴ In addition to N , there are two doublets of Higgs fields \bar{H} and H whose vacuum expectation values give masses to the $T_{3L} = +\frac{1}{2}$ and $T_{3L} = -\frac{1}{2}$ fermions, respectively. Although there is a replication of the fields N , \bar{H} , and H in each of the generations, we can always work in a basis where only one set of N , \bar{H} , and H develop vacuum expectation values, $n/\sqrt{2}$, $\bar{v}/\sqrt{2}$, and $v/\sqrt{2}$, respectively.¹⁶ The scalar potential and the mass matrices have been worked out in the literature.^{17,18} In general, this depends on the charge assignment of the extra $\tilde{U}(1)$, but in the limit that $n \gg v$, \bar{v} , the eigenvector for the lightest Higgs boson can be written as

$$H_L = (1 - \gamma^2)^{1/2} (\cos\beta H_R^0 + \sin\beta \bar{H}_R^0) + \gamma N_R \quad (2.1)$$

with $\tan\beta = \bar{v}/v$ and the H_R^0 , \bar{H}_R^0 , and N_R denoting the real parts of the H^0 , \bar{H}^0 , and N . In Eq. (2.1), $\gamma^2 \ll 1$ as long as $M_{Z^0} \gg M_Z$ as will be assumed in the rest of this paper.¹² The couplings of H_L to the usual Z^0 boson and the boson of the extra $\tilde{U}(1)$ group can be readily written as

$$\begin{aligned} \mathcal{L} = & 2g_Z \sin\theta_W M_Z \sqrt{1 - \gamma^2} (\tilde{Q}_H \cos^2\beta - \tilde{Q}_{\bar{H}} \sin^2\beta) Z_\mu Z'^\mu H_L + \frac{1}{2} g_Z M_Z \sqrt{1 - \gamma^2} Z_\mu Z^\mu H_L \\ & + g_Z^2 \sin^2\theta_W \left[\frac{2M_Z}{g_Z} \sqrt{1 - \gamma^2} (\tilde{Q}_{\bar{H}}^2 \sin^2\beta + \tilde{Q}_H^2 \cos^2\beta) + \tilde{Q}_N^2 n \gamma \right] Z'_\mu Z'^\mu H_L. \end{aligned} \quad (2.2)$$

In Eq. (2.2), \tilde{Q} are the $\tilde{U}(1)$ charges of H , \bar{H} , and N , and $g_Z \equiv g/\cos\theta_W$, where g is the $SU(2)$ gauge coupling. Equation (2.2) can now be used to derive the couplings of H_L to the mass eigenstates. For $n \gg v$, \bar{v} the mixing

between the Z^0 and Z'^0 bosons can be neglected for our purposes. Then Z'^0 is a mass eigenstate with mass $M_{Z'^0} = \tilde{Q}_N^2 g_Z^2 \sin^2\theta_W n^2$ and a coupling to the Higgs boson given by the first term in Eq. (2.2).

The charges \tilde{Q} that appear in Eq. (2.2) are, in general, model dependent. If we assume that E_6 is directly broken to the low-energy group without any intermediate scale, the embedding of $\tilde{U}(1)$ is unique³ and we have $\tilde{Q}_H = -\frac{1}{6}$, $\tilde{Q}_{\bar{H}} = -\frac{2}{3}$, and $\tilde{Q}_N = \frac{5}{6}$. All the $U(1)$ coupling constants are $g' = g \tan\theta_W$. If intermediate scales are allowed, $\tilde{U}(1)$ may be embedded differently so that the \tilde{Q} values may be quite different. As an illustration we may consider the model with the Y' hypercharge considered in Ref. 7. In this model, a large Majorana mass is allowed for ν^c and, hence, this model allows a possible solution for the neutrino mass problem. The charges \tilde{Q} are given by $\tilde{Q}_H = -3/\sqrt{24}$, $\tilde{Q}_{\bar{H}} = -2/\sqrt{24}$, and $\tilde{Q}_N = 5/\sqrt{24}$. We now turn to our predictions for the decay rate for $Z^{0'} \rightarrow Z^0 + H_L$.

In order to discuss this, we first have to fix the various parameters that enter Eq. (2.2). Since we are primarily interested in the case $M_{Z_2} \gg M_Z$ (or equivalently $n \gg \nu, \bar{\nu}$), $\gamma \lesssim 0.3$ ¹² so that $(1 - \gamma^2)^{1/2} \simeq 1$. Furthermore, in the class of models we are considering, $\tan\beta \geq 1$ (Refs.

6 and 7). For the model of Ref. 6, since $|\tilde{Q}_{\bar{H}}| > |\tilde{Q}_H|$ this means that the coupling never vanishes for any value of β . If gaugino masses are the dominant source of SUSY breaking, the favored values of β tend to be large ($\tan\beta \simeq 2.5$) so that the effect of cancellation between the \tilde{Q}_H and $\tilde{Q}_{\bar{H}}$ terms is rather small. On the other hand, for the model of Ref. 7, $|\tilde{Q}_H| > |\tilde{Q}_{\bar{H}}|$ so that the $H_L Z^0 Z^{0'}$ coupling vanishes for $\tan^2\beta = \tilde{Q}_H / \tilde{Q}_{\bar{H}} = \frac{3}{2}$. This introduces a large uncertainty in the cross section for $Z^0 + H_L$ production.

Yet another uncertainty in the branching fraction for $Z^{0'} \rightarrow Z^0 + H_L$ comes from the number of exotics that can be produced by $Z^{0'}$ decay. If all the members of each of the three generations of 27 can be produced without phase-space suppression in $Z^{0'}$ decays, the total $Z^{0'}$ width is increased¹⁹ by a factor ~ 4 so that the $Z^0 + H_L$ cross section is suppressed by the same factor.

The partial width $\Gamma(Z_2 \rightarrow Z_1 + H_L)$ can be readily computed from the couplings in Eq. (2.2). We find

$$\Gamma(Z_2 \rightarrow Z_1 + H_L) = \frac{1}{48\pi} \frac{A^2}{M_{Z_2}^3} \left[2 + \frac{(M_{Z_2}^2 + M_{Z_1}^2 - M_{H_L}^2)^2}{4M_{Z_2}^2 M_{Z_1}^2} \right] \lambda^{1/2}(M_{Z_2}^2, M_{Z_1}^2, M_{H_L}^2), \quad (2.3)$$

where A is the magnitude of the $Z_2^0 Z_1^0 H_L$ coupling which can be read off from Eq. (2.2). The function λ is given by

$$\lambda(x, y, z) = x^2 + y^2 + z^2 - 2xy - 2yz - 2zx. \quad (2.4)$$

Equation (2.3) has been written so as to allow for general mixing between Z^0 and $Z^{0'}$. In the zero-mixing limit we have considered in this paper, $Z_2 = Z^{0'}$, $Z_1 = Z^0$, and

$$A = 2g_Z \sin\theta_W M_Z \sqrt{1 - \gamma^2 (\tilde{Q}_H \cos^2\beta - \tilde{Q}_{\bar{H}} \sin^2\beta)}.$$

The cross section for $Z^0 + H_L$ production by pp collisions at $\sqrt{s} = 40$ TeV is shown in Fig. 1 as a function of the $Z^{0'}$ mass for the model of Ref. 6. We note the following features.

(i) Except near the kinematic threshold, the cross section is rather insensitive to the Higgs-boson mass.

(ii) The cross section is sensitive to $\bar{\nu}/\nu (= \tan\beta)$. In this model it increases with β and is over five times larger for $\beta = 80^\circ$ as compared with $\beta = 45^\circ$. The real situation is probably somewhere in between.

(iii) In order to illustrate the effect of the opening up of the decays of $Z^{0'}$ into the exotic fermions of E_6 , we have also shown the $Z^0 + H_L$ production cross section for the case when $Z^{0'}$ decays into all the exotic fermions of three generations for $\beta = 45^\circ$. As we have discussed, this depresses the cross section by about four as is seen in the lowest curve in the figure.

(iv) For comparison we also show the standard-model $Z^0 t\bar{t}$ background where we have required $M_{t\bar{t}} = 100 \pm 15$ GeV and have assumed that the invariant mass of the $Z^0 t\bar{t}$ system can be measured with a precision of 5%. In this case, the background is smaller than the signal even in the most pessimistic case [see (iii) above] unless

$M_{Z'} < 430$ GeV. The effect of varying these resolutions will be discussed in Sec. V.

If we take all model uncertainties into account, in models where E_6 breaks directly to a rank-5 group, the

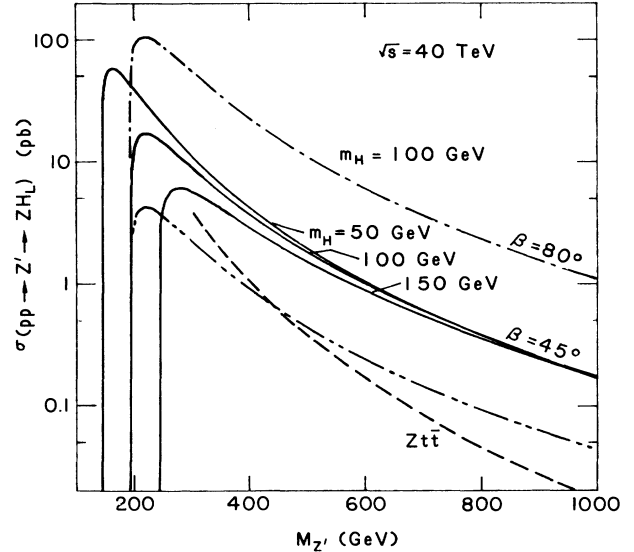


FIG. 1. Total cross section for $pp \rightarrow Z^{0'} \rightarrow Z^0 H_L$ at $\sqrt{s} = 40$ TeV as a function of $M_{Z'}$ for the model of Ref. 6. In all but the lowest dashed-double-dotted curve, the exotic decays of the $Z^{0'}$ are supposed to be kinematically forbidden. The dashed curve shows the standard-model background to $Z^0 t\bar{t}$ production, with $M_{t\bar{t}} = 100 \pm 15$ GeV and $M_{Z t\bar{t}} = M_{Z'} \pm 5\%$. For both signal and background we imposed a rapidity cut $|y| < 4$ on the Z , t , and \bar{t} . We used the Eichten-Hinchliffe-Lane-Quigg parametrization of the parton distributions and $m_t = 40$ GeV.

$Z^0 + H_L$ production cross section is known only up to a factor ~ 25 . We note that $Z^{0'}$ cannot decay into gauginos or gauge bosons, at least in the limit of no mixing with the Z^0 . It could decay into the Higgs-fermion components of the mass eigenstates of the gauge-Higgs-fermion system, but that uncertainty is included in the factor ~ 25 just discussed. We have also assumed that the decay of $Z^{0'}$ into the supersymmetric partners of quarks and leptons is kinematically forbidden.

For the model of Ref. 7, the $Z^0 + H_L$ cross section is, in general, smaller than shown in the figure. The relative suppression can easily be worked out by inserting the appropriate values of $\tilde{U}(1)$ charges. For example, if $\beta = 45^\circ$ it is just $\frac{1}{6}$ of that shown in Fig. 1. As we have already mentioned, the $Z^0 + H_L$ cross section can vanish in this model.

As a guide to the magnitude of the $Z^0 + H_L$ cross section, we will take the $\beta = 45^\circ$ curves shown in Fig. 1. This may well be a realistic value of the cross section since the increase in cross section due to higher, and presumably more realistic, values of β is compensated by the decrease in the branching fraction for $Z^{0'} \rightarrow Z^0 + H_L$ due to additional $Z^{0'}$ channels being open. We then see that for a $Z^{0'}$ mass between 400 and 750 GeV, the $Z^0 + H_L$ cross section varies between 4 and 0.4 pb corresponding to $4 \times 10^4 - 4 \times 10^3$ $Z^0 + H_L$ pairs per year at the SSC. This event rate may well be higher by as much as a factor of 5.

III. THE DECAYS OF THE LIGHT HIGGS BOSON

As we have discussed in the Introduction, in superstring models without any intermediate scale, H_L can have a mass up to ~ 170 GeV. It is, therefore, quite likely that the decay $H_L \rightarrow t\bar{t}$ is kinematically allowed. If H_L can decay only to the usual quarks and leptons, the $t\bar{t}$ mode would dominate and, thus, the $t\bar{t} Z^0$ final state would be the only accessible signal for $Z^{0'} \rightarrow Z^0 + H_L$. In SUSY models, however, the Higgs bosons couple to the gauge-Higgs-fermion sector via gauge interactions and so it is possible for the Higgs boson to decay into the charged (\tilde{W}) and neutral (\tilde{Z}_i) mass eigenstates of this sector with substantial branching fractions. Furthermore, the Higgs scalars also have direct gauge couplings (via D -term interactions) to scalar-quark and scalar-lepton pairs so that the decays $H_L \rightarrow \tilde{q}\tilde{q}$ or $\tilde{l}\tilde{l}$ may be possible. A study of the supersymmetric decay modes of the Higgs boson in superstring-motivated models forms the subject of this section.

We first consider the couplings of the Higgs boson to the gauge-Higgs-fermion sector of the theory. This sector consists of 12 neutral and 4 charged fermions that can mix to produce the chargino and neutralino eigenstates. The charged sector contains the SU(2) gaugino and one charged-Higgs-fermion combination for each of the three generations, whereas the neutralino sector contains the SU(2), U(1), and $\tilde{U}(1)$ gauginos and one set of field H , \bar{H} , and N for each generation.^{6,7,16,17} If, as discussed in Sec. II, we work in a basis where only one set

of the fields \bar{H} , H , and N develop vacuum expectation values (VEV's), the charged sector breaks up into two disconnected sectors; the gauginos mix only with the Higgs-fermion fields that develop VEV's so that the diagonalization^{16,17} is as usual SU(2) \times U(1) supergravity grand unified theories (GUT's). In the same basis, the neutralino sector also splits into two disconnected sectors, with the gauginos mixing only with the neutral doublets and singlets whose scalar partners develop a VEV; i.e., the relevant part of the neutralino mass matrix is 6×6 (Refs. 16 and 17). If, as assumed in this paper, $n \gg v, \bar{v}$ (so that $M_{Z'} \gg M_Z$) the $\tilde{U}(1)$ gaugino and the field N also decouple and we are left with a 4×4 matrix for the SU(2) and U(1) neutral gauginos and the two neutral Higgs fermions \tilde{H}^0 and $\bar{\tilde{H}}^0$.

The resulting 2×2 chargino mass matrix and the 4×4 neutralino mass matrix have the same form as in usual SUSY theories except that the Higgs-fermion mass term arises from the term $\lambda \bar{H} H N$ in the superpotential when N develops a VEV. The diagonalization of the charged sector can be done analytically and has been considered by several authors.²⁰ The neutral sector has to be diagonalized numerically. Here we present the relevant couplings of the scalar H_L to the mass eigenstates of the gauge-Higgs-fermion system in terms of their eigenvector components using the notation of Ref. 21.

The couplings to the charginos come only from the H and \bar{H} content of H_L [see Eq. (2.1)] whereas the coupling to the neutral sector can in principle also involve the singlet component N . The latter would couple only to the N fermion and the $\tilde{U}(1)$ gaugino. Since the amount of the N fermion and the $\tilde{U}(1)$ gaugino in the light neutralinos is negligible, we ignore this contribution to the coupling. The Lagrangian relevant for the two-body decays of H_L then takes the form²²

$$\mathcal{L} = \sqrt{1 - \gamma^2} H_L \left\{ \frac{1}{2} g \sum_f \frac{m_f}{M_W} \bar{f} f + g \sqrt{2} S \bar{W} \tilde{W} + \sum_{i,j} X^{ij} \bar{\tilde{Z}}_i (-i\gamma_5)^{\theta_i + \theta_j} \tilde{Z}_j \right\}, \quad (3.1)$$

where i, j label the various (Majorana) mass eigenstates of the neutralino system and f is any quark or lepton. In Eq. (3.1), the constants S and X^{ij} are known in terms of the eigenvectors and are given by

$$S = \frac{1}{2} (-1)^{\theta} (-\cos\beta \cos\gamma_L \sin\gamma_R + \sin\beta \cos\gamma_R \sin\gamma_L), \quad (3.2)$$

$$X^{ij} = (-1)^{\theta_i + \theta_j + 1} \frac{1}{2} (v_2^{(i)} \cos\beta - v_1^{(i)} \sin\beta) (g v_3^{(j)} - g' v_4^{(j)}). \quad (3.3)$$

Here $\theta_i = 0$ (1) if the \tilde{Z}_i has a positive (negative) eigenvalue in the mass matrix and $\theta_- = 0$ (1) if the \tilde{W} has a positive (negative) eigenvalue in the chargino mass matrix. Finally, $v_1^{(i)}$, $v_2^{(i)}$, $v_3^{(i)}$, and $v_4^{(i)}$ are the \bar{H} , H , SU(2) and U(1) gauge fermion components in \tilde{Z}_i . The coefficients $v_j^{(i)}$ are obtained numerically. Analytic expressions for γ_L and γ_R in terms of the parameters that enter the mass matrix may be found in Ref. 21 (see Ref. 23).

In our computations we assume a common gaugino mass at the unification scale so that the SU(3), SU(2), and U(1) gaugino masses μ_i are related by

$$\frac{3}{5} \frac{\mu_1}{\alpha_1} = \frac{\mu_2}{\alpha_2} = \frac{\mu_3}{\alpha_3} \quad (3.4)$$

with α_i being the fine-structure constants of the appropriate component of the gauge group. Thus, only one of the gaugino masses is an independent parameter. We take this to be gluino mass $m_{\tilde{g}} = |\mu_3|$. Our inputs at the scale M_W are fixed by $\alpha_{EM} = \frac{1}{128}$, $\sin^2\theta_W = 0.22$, and $\alpha_3 = 0.136$ corresponding to six flavors of quarks with $\Lambda = 0.2$ GeV.

$$\Gamma(H_L \rightarrow \tilde{Z}_i \tilde{Z}_j) = \frac{\Delta_{ij}(1-\gamma^2)(X_{ij}+X_{ji})^2}{8\pi m_H^3} \{m_H^2 - [m_{\tilde{Z}_i} + (-1)^{\theta_i+\theta_j} m_{\tilde{Z}_j}]^2\} \lambda^{1/2}(m_H^2, m_{\tilde{Z}_i}^2, m_{\tilde{Z}_j}^2), \quad (3.7)$$

where N_C in Eq. (3.5) is 1 (3) if f is a lepton (quark), $\Delta_{ij} = 1, (\frac{1}{2})$ if \tilde{Z}_i and \tilde{Z}_j are different (the same) neutralinos and the function λ in Eq. (3.7) is as defined in Eq. (2.4).

The masses and couplings of \tilde{W} and \tilde{Z}_i are all fixed in terms of three parameters, $m_{\tilde{g}}$, the angle β , and the effective $H\tilde{H}$ mass term $\lambda n/\sqrt{2} \equiv \epsilon$. The value of n is fixed by the Z^0 mass, but the value of λ is essentially free except for upper bounds.¹² Perturbative unification without intermediate scales implies $\lambda < 0.95$ (for a top quark ~ 40 GeV) corresponding to $m_H \lesssim 170$ GeV. If SUSY breaking is dominantly due to gaugino masses, the upper bound on λ moves down to 0.35 yielding¹⁷ $m_H < 110$ GeV. In models with an intermediate scale $\sim 10^{10}$ GeV, λ values up to 1.2 ($m_H < 220$ GeV) are allowed.¹² In principle, therefore, the Higgs-fermion mass term is independent of $M_{Z'}$. For $M_{Z'} \sim 0.5$ TeV, ϵ substantially exceeds M_W unless λ is very small. For illustrative purposes, we have chosen $4M_W$ as a typical value of ϵ . The effects of varying ϵ will be discussed shortly.

The branching fractions for H_L decays into top quarks, \tilde{W} pairs and $\tilde{Z}_i \tilde{Z}_j$ pairs are shown in Fig. 2 as a function of the gluino mass. For definiteness we have fixed the Higgs-boson mass to be 130 GeV and the top-quark mass to be 40 GeV. The branching fractions are shown for $\tan\beta = +1, +3, -1,$ and -3 . The minimum gluino mass in each of the cases is shown so that $m_{\tilde{W}} \gtrsim 35$ GeV as is implied by the CERN Sp \bar{p} S collider data.²⁴ For each value of $\tan\beta$, ϵ and $m_{\tilde{g}}$, the chargino and neutralino mass matrices have been diagonalized to obtain the masses and the coupling. The partial widths and the resulting branching fractions have then been computed from Eqs. (3.5)–(3.7). The decay width into bottom-quark pairs, though not shown, has been included in the computation.

We see that the branching fractions into the \tilde{W} and \tilde{Z} modes can be substantial when these are kinematically allowed. Although the particular value of $m_{\tilde{g}}$ at which the supersymmetric decays of H_L are kinematically

The partial widths for H_L to decay into fermion pairs, \tilde{W} pairs and $\tilde{Z}_i \tilde{Z}_j$ can now be computed using the couplings in Eq. (3.1). We find

$$\Gamma(H_L \rightarrow f\bar{f}) = \frac{g^2}{32\pi} N_C \frac{m_f^2}{M_W^2} (1-\gamma^2) \left[1 - \frac{4m_f^2}{m_H^2}\right]^{3/2} m_H, \quad (3.5)$$

$$\Gamma(H_L \rightarrow \tilde{W}\tilde{W}) = \frac{g^2}{4\pi} S^2 (1-\gamma^2) \left[1 - \frac{4m_{\tilde{W}}^2}{m_H^2}\right]^{3/2} m_H, \quad (3.6)$$

and

suppressed depends on $\tan\beta$, these decays are important for an interesting range of gluino masses. Of course, this range increases with m_H .

We see that the supersymmetric decays of H_L may contribute as much as half of its decay width at least for $\epsilon = 4M_W$. This, of course, leads to the possibility of interesting new signatures for the intermediate-mass Higgs boson. The supersymmetric modes are maximal for $\tan\beta = 1$ and are strongly dependent on the relative sign of $\tan\beta$ and ϵ . (A simultaneous change of the signs of $\tan\beta$ and ϵ leaves the branching fractions of H_L unaltered.²⁵) We note here that for the values of $\tan\beta$ favored by the model of Ref. 6, the SUSY decay modes are the smallest of the four cases shown in the figure [see Fig. 2(d)].

We now turn to the dependence of the Higgs-boson branching fractions on ϵ , shown in Fig. 3 for fixed values $m_{\tilde{g}} = 300$ GeV and $\tan\beta = 1$. In order to understand this dependence, we recall that the couplings of the Higgs boson to the gauge-Higgs-fermion system arise from the Higgs-boson–Higgs-fermion–gaugino coupling. The coupling of H_L to the two mass eigenstates arises from the gaugino content of one and the Higgs-fermion content of the other. This structure is clearly reflected in Eq. (3.2) where $\sin\gamma$ and $\cos\gamma$ are the gaugino and Higgs-fermion components of \tilde{W} , and in Eq. (3.3) where the components $v_1^{(i)}$ and $v_2^{(i)}$ refer to the Higgs-fermion components of \tilde{Z}_i whereas $v_3^{(i)}$ and $v_4^{(i)}$ denote its gaugino components.²¹ For values of ϵ much larger than M_W , the SU(2) and U(1) gauginos are (almost) the two lightest eigenstates (for the values of gaugino masses considered here), so that the couplings of these to H_L exist only by virtue of the small Higgs-fermion content of \tilde{Z}_1 and \tilde{Z}_2 . Because this Higgs-fermion content falls off as $1/\epsilon$ for large ϵ , the supersymmetric decays of H_L become unimportant, as seen in Fig. 3, although they may be kinematically allowed. For smaller values of ϵ , these decays become very important. As can be seen in Fig. 3, for $\epsilon = 200$ GeV, $m_{\tilde{g}} = 300$ GeV, and $\tan\beta = 45^\circ$ (corre-

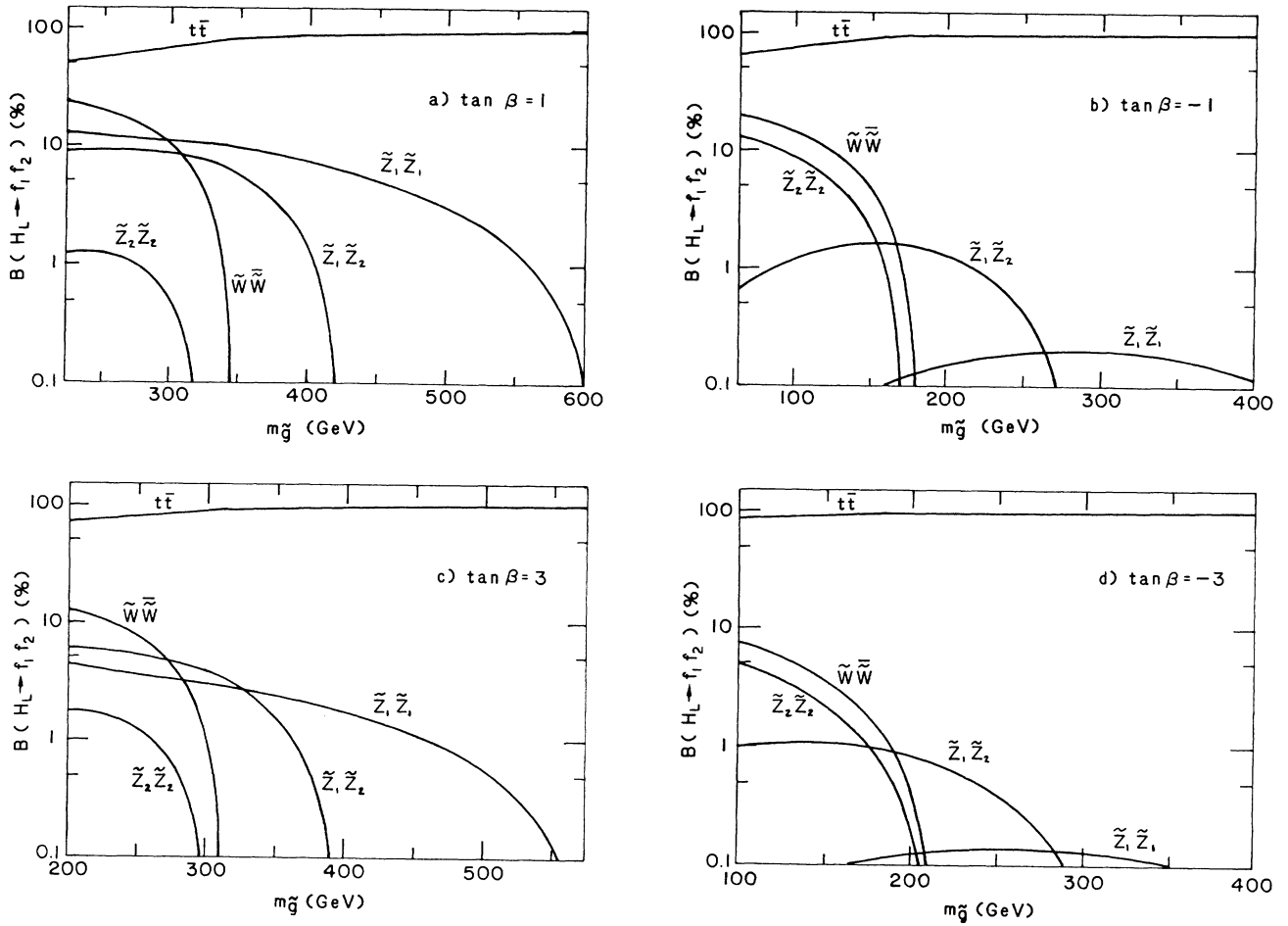


FIG. 2. Branching fractions for H_L decays as a function of the gluino mass, for $m_H = 130$ GeV, $m_t = 40$ GeV, $\epsilon = 4M_W$. The decay $H_L \rightarrow b\bar{b}$, though not shown in the figure, was taken into account for the computation of the total decay width of H_L . The minimal gluino mass is chosen such that $m_{\tilde{W}} = 35$ GeV.

sponding to $m_{\tilde{W}} = 35$ GeV), the width into the $\tilde{W}\tilde{W}$ mode even exceeds that into the $t\bar{t}$ mode.

Before closing this section we should point out that the D terms induce model-dependent couplings of Higgs scalars to scalar-fermion pairs. In this paper we have assumed that all the scalar quarks and leptons are too heavy to be produced via H_L decays. It is perfectly possible that the scalar neutrinos ($\tilde{\nu}_L$) may be light²⁶ and yet have escaped experimental detection.²⁷ The D -term coupling of H_L to $\tilde{\nu}_L\tilde{\nu}_L$ pairs from the usual $SU(2) \times U(1)$ exactly vanishes, but that from $\tilde{U}(1)$ does not. Although the coupling is model dependent, we have checked that it is bounded from above so that the branching fraction for this decay cannot be much above 7.5% per generation although it may be very small. We will neglect this decay in the rest of this paper. However, we note that scalar-neutrino (and other scalar-quark and -lepton) pairs couple to the heavier Higgs scalars even via the D terms of the usual $SU(2) \times U(1)$ and may be important for their decays.

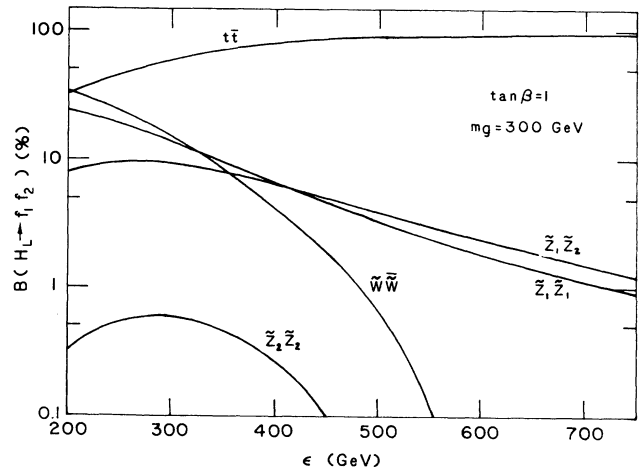


FIG. 3. Branching fractions for H_L decays as a function of ϵ for $m_{\tilde{g}} = 300$ GeV. Values of the other parameters and notations are as in Fig. 2.

IV. THE DECAYS OF \tilde{W} AND \tilde{Z}_2

In order to classify the signals resulting from H_L decays, we need to know the branching fractions for the decays of \tilde{W} and \tilde{Z}_2 . These decay into a lepton-scalar-lepton or a quark-scalar-quark pair if these decays are kinematically allowed. Otherwise, they decay via three-body modes,²⁰ $\tilde{W} \rightarrow l\bar{\nu}\tilde{Z}_1$ or $q\bar{q}'\tilde{Z}_1$, and $\tilde{Z}_2 \rightarrow l\bar{l}\tilde{Z}_1$, $q\bar{q}\tilde{Z}_1$ or $\nu\bar{\nu}\tilde{Z}_1$, which are mediated by virtual gauge bosons or virtual scalar quarks or scalar leptons. The decay $\tilde{Z}_2 \rightarrow \nu\bar{\nu}\tilde{Z}_1$ is severely suppressed if $\tilde{Z}_1 \approx \tilde{\gamma}$. The decays $\tilde{Z}_2 \rightarrow u\bar{d}\tilde{W}$ or $l\bar{\nu}\tilde{W}$, which are mediated by virtual W exchange, can be important in some cases, as will be discussed later. The branching fractions are rather model dependent and it is the study of these that forms the subject of this section.

As we have discussed in the last section, the Higgs-fermion mass term which comes from the VEV of the singlet field substantially exceeds M_W . For the range of \tilde{W} , \tilde{Z}_1 , and \tilde{Z}_2 masses such that the decays of H_L into these are kinematically allowed, the SU(2) and U(1) gaugino masses cannot be too large. In this case, the Higgs-fermion content of these lighter-mass eigenstates is at most a few percent.^{20,21} This means that the coupling of the Z^0 to the neutralino states \tilde{Z}_1 and \tilde{Z}_2 are suppressed by *two* factors of the (small) Higgs-fermion mixing in the neutralino mass eigenstates [recall that couplings of Z^0 to neutral gauge-fermion components are forbidden by SU(2)×U(1)]. Thus for the relevant choice of parameters, the $Z^0\tilde{Z}_i\tilde{Z}_j$ ($i, j = 1, 2$) couplings are only $\sim 10^{-3}$ – 10^{-2} of the $Z^0\tilde{W}\tilde{W}$ or $W\tilde{W}\tilde{Z}_i$ couplings which are of normal gauge strength. We can therefore neglect the virtual Z^0 contributions to the de-

cays $\tilde{Z}_2 \rightarrow f\bar{f}\tilde{Z}_1$ (here f denotes a quark or lepton).

The couplings that enter the computation of the decays of \tilde{W} and \tilde{Z}_2 may be found in Ref. 21 except for the couplings of \tilde{W} and \tilde{Z}_i to the leptons. The couplings of \tilde{W} to leptons are obviously the same as to the quarks with the replacement $u \rightarrow \nu$ and $d \rightarrow l$. The $\tilde{Z}_i\bar{l}l$ and $\tilde{Z}_i\nu\bar{\nu}$ couplings are given by ($f = l, \nu$)

$$\mathcal{L}_{\tilde{Z}_i f \bar{f}} = i A_{\tilde{Z}_i}^f \bar{f}_L^\dagger \tilde{Z}_i \frac{1 - \gamma_5}{2} f + i B_{\tilde{Z}_i}^f \bar{f}_R^\dagger \tilde{Z}_i \frac{1 + \gamma_5}{2} f + \text{H.c.}, \quad (4.1)$$

$$A_{\tilde{Z}_i}^l = -(i)^{\theta_i - 1} (-1)^{\theta_i + 1} \left[\frac{g}{\sqrt{2}} v_3^{(i)} + \frac{g'}{\sqrt{2}} v_4^{(i)} \right], \quad (4.2a)$$

$$A_{\tilde{Z}_i}^\nu = (i)^{\theta_i - 1} (-1)^{\theta_i + 1} \left[\frac{g}{\sqrt{2}} v_3^{(i)} - \frac{g'}{\sqrt{2}} v_4^{(i)} \right], \quad (4.2b)$$

$$B_{\tilde{Z}_i}^l = -(i)^{\theta_i - 1} \sqrt{2} g' v_4^{(i)}, \quad (4.2c)$$

and

$$B_{\tilde{Z}_i}^\nu = 0. \quad (4.2d)$$

The notation is as defined in the discussion following Eq. (3.3). The partial width for the decay $\tilde{Z}_2 \rightarrow f\bar{f}\tilde{Z}_1$ can now be readily calculated. We find

$$\Gamma(\tilde{Z}_2 \rightarrow \tilde{Z}_1 f \bar{f}) = \frac{1}{2m_{\tilde{Z}_2}} \frac{1}{(2\pi)^5} \left(\frac{1}{2} |M_L|^2 + \frac{1}{2} |M_R|^2 \right) N_C \quad (4.3)$$

with

$$\frac{1}{2} |M_L|^2 = 2 |A_{\tilde{Z}_1}^f|^2 |A_{\tilde{Z}_2}^f|^2 [\psi(m_{\tilde{Z}_2}, m_{\tilde{f}_L}, m_{\tilde{Z}_1}) + (-1)^{\theta_1 + \theta_2} \varphi(m_{\tilde{Z}_2}, m_{\tilde{f}_L}, m_{\tilde{Z}_1})] \quad (4.4a)$$

and

$$\frac{1}{2} |M_R|^2 = 2 |B_{\tilde{Z}_1}^f|^2 |B_{\tilde{Z}_2}^f|^2 [\psi(m_{\tilde{Z}_2}, m_{\tilde{f}_R}, m_{\tilde{Z}_1}) + (-1)^{\theta_1 + \theta_2} \varphi(m_{\tilde{Z}_2}, m_{\tilde{f}_R}, m_{\tilde{Z}_1})]. \quad (4.4b)$$

In Eq. (4.3), $N_C = 1$ (3) if f is a lepton (quark). The functions ψ and φ in Eq. (4.4) are as defined in Eq. (3.2) of Ref. 21. Finally, the partial widths for the decay of \tilde{W} have been obtained by numerically integrating the spin-averaged squared matrix element, which reads, in the notation of Ref. 21,

$$\begin{aligned} \frac{1}{2} |M(\tilde{W} \rightarrow d\bar{u}\tilde{Z}_1)|^2 = & \frac{1}{2} \left[|A_{\tilde{W}}^d|^2 |A_{\tilde{Z}_1}^u|^2 \frac{4\tilde{W} \cdot d \tilde{Z}_1 \bar{u}}{D_{\bar{u}}^2} + |A_{\tilde{W}}^u|^2 |A_{\tilde{Z}_1}^d|^2 \frac{4\bar{u} \cdot \tilde{W} d \cdot \tilde{Z}_1}{D_d^2} \right. \\ & + \frac{8g^4}{D_W^2} [(|X_{(-)}^1|^2 + |Y_{(-)}^1|^2)(\tilde{W} \cdot \bar{u} \tilde{Z}_1 \cdot d + \tilde{W} \cdot d \tilde{Z}_1 \cdot \bar{u}) - (|X_{(-)}^1|^2 - |Y_{(-)}^1|^2)m_{\tilde{W}}m_{\tilde{Z}_1} \\ & + 2X_{(-)}^1 Y_{(-)}^1 (\tilde{W} \cdot \bar{u} \tilde{Z}_1 \cdot d - \tilde{W} \cdot d \tilde{Z}_1 \cdot \bar{u})] + 4 \text{Re}(A_{\tilde{W}}^u A_{\tilde{W}}^d A_{\tilde{Z}_1}^{u*} A_{\tilde{Z}_1}^{d*}) \frac{m_{\tilde{W}} m_{\tilde{Z}_1}}{D_{\bar{u}} D_d} \bar{u} \cdot d \\ & - \frac{\sqrt{2}g^2 \text{Re}[(-i)^{\theta_1} A_{\tilde{W}}^u A_{\tilde{Z}_1}^{d*}]}{D_{\bar{u}} D_W} 4[2(X_{(-)}^1 + Y_{(-)}^1) \bar{u} \cdot \tilde{W} d \cdot \tilde{Z}_1 - m_{\tilde{W}} m_{\tilde{Z}_1} (X_{(-)}^1 - Y_{(-)}^1) \bar{u} \cdot d] \\ & \left. + \frac{\sqrt{2}g^2 \text{Re}[(-i)^{\theta_1} A_{\tilde{W}}^d A_{\tilde{Z}_1}^{u*}]}{D_{\bar{u}} D_W} 4[2(X_{(-)}^1 - Y_{(-)}^1) d \cdot \tilde{W} \bar{u} \cdot \tilde{Z}_1 - m_{\tilde{W}} m_{\tilde{Z}_1} (X_{(-)}^1 + Y_{(-)}^1) \bar{u} \cdot d] \right] \quad (4.5) \end{aligned}$$

where the denominators are given by

$$D_{\bar{u}} = (\tilde{W} - \bar{d})^2 - m_{\bar{u}_L}^2, \quad (4.6a)$$

$$D_{\bar{d}} = (\tilde{W} - u)^2 - m_{\bar{d}_L}^2, \quad (4.6b)$$

and

$$D_W = (\tilde{W} - \tilde{Z}_1)^2 - M_W^2. \quad (4.6c)$$

In Eqs. (4.5) and (4.6), the particle labels denote the four-momenta of the particles. The corresponding matrix element for the leptonic decays of \tilde{W} can be obtained from Eq. (4.5) via the substitution $u \rightarrow \nu$ and $d \rightarrow l$. We note that the color factor has not been included in Eq. (4.5).

The decay widths depend on the scalar-quark and -lepton masses. In E_6 supergravity GUT's, these are given by²⁸

$$m_{e_L}^2 = m_0^2 + 0.384m_g^2 - 0.27 \cos(2\beta)M_Z^2 + a_L M_Z^2, \quad (4.7a)$$

$$m_{e_R}^2 = m_0^2 + 0.138m_g^2 - 0.23 \cos(2\beta)M_Z^2 + a_R M_Z^2, \quad (4.7b)$$

$$m_{\bar{\nu}_L}^2 = m_0^2 + 0.384m_g^2 + 0.5 \cos(2\beta)M_Z^2 + a_L M_Z^2, \quad (4.7c)$$

$$m_q^2 \simeq m_0^2 + 3.6m_g^2. \quad (4.7d)$$

Here m_0 is a common supersymmetry-breaking scalar mass and the gluino mass m_g is equal to the universal gaugino mass $m_{1/2}$ at the unification scale. The last two terms in Eqs. (4.7a)–(4.7c) come from the $SU(2) \times U(1)$ and $\tilde{U}(1)$ D terms, whereas the second term comes from the renormalization of the masses from the unification

scale down to the weak scale. The $\tilde{U}(1)$ D terms obviously depend on the $\tilde{U}(1)$ charges of the particles and hence are model dependent. Again assuming $n \gg \nu, \bar{\nu}$, the coefficients a_L and a_R are given by -0.1 and 0.2 , respectively, for the model of Ref. 6, whereas for that of Ref. 7 we have $a_L = 0.2$ and $a_R = 0.1$. We note that in Eq. (4.7d) we have neglected the D terms for the scalar quarks in comparison with the other terms. We have also neglected the small difference in the evolution of the masses (the second term) in the two models.

The ratio of m_0 to $m_{1/2}$ depends on the mechanism for supersymmetry breaking which, it is fair to say, is not yet understood. Some authors^{6,29} have argued that gaugino masses are the dominant source of SUSY breaking so that $m_0 \approx 0$, whereas nonzero scalar masses (≤ 1 TeV) have been suggested by other authors.³⁰ In the absence⁷ of a clear understanding of the mechanism for supersymmetry breaking, we have assumed that gaugino and scalar masses are about equal at the unification scale so that in the calculation of the mass spectrum we assume $m_0 = m_g$. This is the only place where this assumption is used in the paper.

Before proceeding with the numerical computation of the branching fractions, we note that if the scalar-quark and -lepton masses are all very large ($\gg M_W$), the decays $\tilde{Z}_2 \rightarrow l\nu\tilde{W}$ and $u\bar{d}\tilde{W}$, which can be mediated by virtual W 's as well as virtual scalar leptons or scalar quarks, may be important³¹ since the $W\tilde{Z}_2\tilde{W}$ vertex is not suppressed by small mixing angles. This decay is only important when the smallness of the phase space for the $\tilde{Z}_2 \rightarrow \tilde{W}$ decay is made up by the smaller propagator suppression of the W exchange relative to the scalar-quark or -lepton exchange, i.e., when $M_W \ll m_{q_L}, m_{l_L}, m_{\bar{\nu}_L}$. We have, therefore, retained only the W -exchange contribution in the computation of this decay. The partial width is given by

$$\begin{aligned} \Gamma(\tilde{Z}_2 \rightarrow f\bar{f}'\tilde{W}) &= \frac{1}{2m_{\tilde{Z}_2}} \frac{N_C}{(2\pi)^5} \frac{2\pi^2 g^4}{3} \\ &\times \int dE \frac{\sqrt{E^2 - m_{\tilde{W}}^2}}{(m_{\tilde{Z}_2}^2 + m_{\tilde{W}}^2 - M_W^2 - 2m_{\tilde{Z}_2}E)^2} \\ &\times \{ (|X_{(-)}|^2 + |Y_{(-)}|^2) [3(m_{\tilde{Z}_2}^2 + m_{\tilde{W}}^2)m_{\tilde{Z}_2}E - 4m_{\tilde{Z}_2}^2E^2 - 2m_{\tilde{Z}_2}^2m_{\tilde{W}}^2] \\ &- 3(|X_{(-)}|^2 - |Y_{(-)}|^2)m_{\tilde{Z}_2}m_{\tilde{W}}(m_{\tilde{Z}_2}^2 + m_{\tilde{W}}^2 - 2m_{\tilde{Z}_2}E) \}, \end{aligned} \quad (4.8)$$

where the integral over the \tilde{W} energy E ranges from $m_{\tilde{W}}$ to $(m_{\tilde{W}}^2 + m_{\tilde{Z}_2}^2)/2m_{\tilde{Z}_2}$. Here we have neglected all quark and lepton masses. The conjugate decay, $\tilde{Z}_2 \rightarrow \bar{f}f'\tilde{W}$ also occurs at the same rate.

The branching fractions for \tilde{W} and \tilde{Z}_2 decays can now be computed using Eqs. (4.3)–(4.8). The result for two

typical models^{6,7} is shown in Table I for a range of gaugino masses (m_g) for which the decays $H_L \rightarrow \tilde{W}\tilde{W}$ or $\tilde{Z}_i\tilde{Z}_j$ are significant. We have also restricted our choice of parameters so that the gaugino and scalar masses at the unification scale and the Z^0 mass are all comparable. In our computation, we have assumed that the top

TABLE I. The percentage branching fractions for \tilde{Z}_2 and \tilde{W} decays for the models of Refs. 6 and 7 (in parentheses) with the scalar masses as described in the text. Note that the $\tilde{Z}_2 \rightarrow e^+e^-$ denotes the branching fraction to just electrons so that the total charged-lepton branching fraction is thrice that shown. The $\tilde{Z}_2 \rightarrow \tilde{W}$ branching includes both $\tilde{Z}_2 \rightarrow l\tilde{\nu}\tilde{W}$ and $q\bar{q}'\tilde{W}$ decays. The \tilde{W} branching fraction shown is also for just one family of leptons. The parameters have been chosen so that there is a substantial branching fraction for H_L into the \tilde{W} and \tilde{Z}_i modes. We have also required that $M_{Z'}$ is not very different from the supersymmetry-breaking scale $m_0 = m_{\tilde{g}}$. (The model of Ref. 7 always gives a branching fraction of 11% since the scalar masses are too heavy for the contribution of the graphs mediated by scalar exchanges to be significant.)

$\bar{\nu}/\nu$	$m_{\tilde{g}}$ (GeV)	$m_{\tilde{Z}_1}$ (GeV)	$m_{\tilde{Z}_2}$ (GeV)	$m_{\tilde{W}}$ (GeV)	$M_{Z'}$ (GeV)	\tilde{Z}_2				
						e^+e^-	$\nu\bar{\nu}$	$q\bar{q}$	\tilde{W}	$\tilde{W} \rightarrow e\bar{\nu}\tilde{Z}_1$
-1	100	14	47	44	250	30 (26)	9 (5)	2 (18)		21
-1	200	28	71	69	250	26 (26)	18 (15)	4 (6)		12
-1	200	28	71	69	500	27 (25)	19 (14)	1 (14)		13
+1	200	12	37	29	250	1 (2)	6 (3)	2 (2)	88 (90)	12
+1	400	39	82	77	250	6 (7)	31 (27)	4 (4)	46 (48)	11
+1	200	12	37	29	500	1 (1)	15 (1)	1 (2)	82 (94)	12
+1	400	39	82	77	500	5 (6)	36 (23)	4 (5)	44 (54)	11
-3	100	14	38	36	250	14 (23)	58 (16)	1 (16)		21
-3	200	27	62	61	250	22 (22)	31 (28)	3 (5)		12
-3	200	27	62	61	500	21 (21)	36 (25)	1 (11)		13
+3	200	18	40	37	250	7 (10)	62 (43)	7 (10)	12 (16)	12
+3	400	43	88	86	250	12 (12)	59 (56)	5 (5)	1 (1)	11
+3	200	18	40	37	500	3 (9)	84 (29)	3 (16)	5 (28)	13
+3	400	43	88	86	500	11 (12)	63 (54)	4 (7)	1 (2)	11

quark is too heavy to be produced via \tilde{W} and \tilde{Z}_2 decays.

We see that \tilde{W} typically decays into the leptonic mode with a branching fraction of 11–13% per lepton family. This is because the scalar quarks and leptons are substantially heavier than M_W for most values of $m_{\tilde{g}}$ and $M_{Z'}$, so that the \tilde{W} branching fractions are essentially the same as those of the W boson. An exception to this is the case where $m_{\tilde{g}}$ and $M_{Z'}$ are relatively small, since in this case the masses of \tilde{e}_L and $\tilde{\nu}_L$ are about M_W for the model of Ref. 6. On the other hand, for the model of Ref. 7, the scalar masses are always large (note that the $\tilde{U}(1)$ D terms always increase the mass in this case [see Eqs. (4.7)] so that the W -exchange amplitude dominates).

We now turn to a discussion of \tilde{Z}_2 decays. We see that the sign of $\bar{\nu}/\nu$ (of course, this sign could be absorbed in other entries in the mass matrix; only the relative sign of $\bar{\nu}/\nu$ and $\epsilon\mu_2$ is relevant, so $\bar{\nu}/\nu = -1$ should be understood to mean this relative sign is negative) is an important factor³² in determining the decay pattern of \tilde{Z}_2 . For negative values of $\bar{\nu}/\nu$, \tilde{Z}_2 decays via the W -gaugino (\tilde{W}) mode less than 1% of the time, whereas for positive values of $\bar{\nu}/\nu$, this decay is substantial for both the models considered. This is because $m_{\tilde{Z}_2} - m_{\tilde{W}}$ and hence the partial width for $\tilde{Z}_2 \rightarrow \tilde{W}$ decay is sensitively dependent on the sign in the mass matrix. For $\bar{\nu}/\nu \simeq 1$, this mass difference is largest, and the branching fraction into the \tilde{W} mode may even exceed 90%. We mention here that in our computation of the $\tilde{Z}_2 \rightarrow \tilde{W}$ decays, we have included only the contributions from those amplitudes where the decay is kinematically possible, including masses of 0.5, 1.5, and 1.732 GeV for the strange quark, charmed quark, and τ lepton, respectively. In actual computation of the partial width, however, we have

neglected matter fermion masses so that the $\tilde{Z}_2 \rightarrow \tilde{W}$ branching fractions in Table I are somewhat overestimated. The \tilde{W} branching fractions of the \tilde{Z}_2 are somewhat larger for the model of Ref. 7 as compared with that of Ref. 6, since the larger scalar masses lead to smaller widths for the $\tilde{Z}_2 \rightarrow \tilde{Z}_1$ decays.

For $\bar{\nu}/\nu < 0$, where $\tilde{Z}_2 \rightarrow \tilde{W}$ decays are negligible, the $\tilde{Z}_2 \rightarrow \nu\bar{\nu}\tilde{Z}_1$ and $l\bar{l}\tilde{Z}_1$ decays dominate the hadronic decays since the scalar leptons are much lighter than the scalar quarks. We see that the branching fraction into the charged-lepton modes is substantial (as high as 30% per lepton flavor) with a substantial part of the remainder of the decays being via $\tilde{Z}_2 \rightarrow \nu\bar{\nu}\tilde{Z}_1$. The latter, of course, add to the $Z^0 + \cancel{p}_T$ signal that primarily comes from the invisible $H_L \rightarrow \tilde{Z}_1\tilde{Z}_1$ decay of the Higgs boson. For large positive values of $\bar{\nu}/\nu$, the $\tilde{Z}_2 \rightarrow \nu\bar{\nu}\tilde{Z}_1$ decay dominates the charged-lepton decay. This is, in part, because \tilde{Z}_1 is no longer “photinlike” which it was for $\bar{\nu}/\nu < 0$. For this case the coupling $e\tilde{e}_L\tilde{Z}_1$ is suppressed by mixings in much the same way as $\nu\tilde{\nu}_L\tilde{Z}_1$ is suppressed when $\tilde{Z}_1 \approx \tilde{\gamma}$. Furthermore, in the model of Ref. 6, \tilde{e}_R tends to be heavy due to the large $\tilde{U}(1)$ D term. This accounts for the rather large difference in the branching fractions for the two models. Finally, if the gluino mass is large, the scalar electrons and scalar neutrinos tend to become degenerate so that the difference between the two models is greatly reduced, as can be seen in the $m_{\tilde{g}} = 400$ GeV entries in the table.

To summarize, we see from Table I that for almost the whole range of parameters considered, \tilde{Z}_2 dominantly decays leptonically in both the models. (The one exception to this is the case $\bar{\nu}/\nu = 1$, in which case $\tilde{Z}_2 \rightarrow \tilde{W}$ decays dominate.) This leads to potentially background-free lepton pair + Z^0 events essentially free

from hadronic activity and also to events with $Z^0 + \cancel{p}_T$. The topologies of these events and a discussion of some of the backgrounds forms the subject of the next section.

V. SIGNALS FOR HIGGS BOSONS FROM $Z^{0'}$ DECAYS AT THE SSC

In previous sections we have analyzed the production and subsequent decays of the Higgs boson produced via the decay $Z^{0'} \rightarrow Z^0 + H_L$. We saw that a variety of interesting signals are possible, depending on the parameters of the model. Here we study the backgrounds to these signals, and assess the prospects of discovering the lightest neutral Higgs boson at the SSC. Since we are working within the framework of an E_6 supergravity GUT, we have assumed that the decays of H_L into gauge-boson pairs are kinematically suppressed.¹²

As we have already seen, for a $Z^{0'}$ mass in the vicinity of 0.5 TeV, a typical value in this class of models, as many as 10^4 – 10^5 $Z^0 H_L$ pairs may be annually expected at the SSC. This large event rate allows us to use the clean $Z^0 \rightarrow l^+ l^-$ ($l = e, \mu$) decays as a trigger for the Higgs-boson signal. Our analysis naturally divides up into signals from the standard $t\bar{t}$ decay of the Higgs boson and those from its supersymmetric decays. We consider each of these in turn.

(a) $H_L \rightarrow t\bar{t}$ decays. Assuming that the top quark is not too heavy, the decay $H_L \rightarrow t\bar{t}$ dominates the Higgs-boson decays; thus $Z^0 t\bar{t}$ events, with the mass of the $Z^0 t\bar{t}$ system peaking around $M_{Z'}$ and that of the $t\bar{t}$ subsystem around m_H , would be a signature for the decay $Z^{0'} \rightarrow Z^0 + H_L$. We note here that the $Z^{0'}$, if it exists, will almost certainly be discovered via $Z^{0'} \rightarrow l^+ l^-$ (Ref. 33) so that by the time a search for its Higgs-boson decay mode is carried out, $M_{Z'}$ and $\Gamma_{Z'}$ will be well determined. This will, of course, facilitate the Higgs-boson search and reduce some of the theoretical uncertainty in the prediction of the $Z^0 H_L$ production cross section. We have already seen (see Fig. 1) that the cross section for associated Z^0 –Higgs-boson production is substantial and so the crucial factor in determining whether H_L can be identified at the SSC is the size of the backgrounds to $Z^0 t\bar{t}$ production.

The background dominantly comes from gluon-gluon fusion and quark-antiquark annihilations, with

$M_{Z' t\bar{t}} \sim M_{Z'}$ and $M_{t\bar{t}} \sim m_H$. The former was first computed by Gunion and Kunzst.¹⁴ We have independently evaluated this and also the contribution from $q\bar{q}$ annihilation. For $M_{Z'} \sim 0.5$ TeV, the quark contribution is typically 15–20% of that of the gluons, whereas for $M_{Z'} = 1$ TeV, $q\bar{q}$ annihilation dominates gg fusion by a factor of about 2. The $q\bar{q}$ contribution dominantly comes from the two Feynman diagrams where the Z^0 is radiated off the initial quarks; the two diagrams where the Z^0 is radiated off the final t -quark lines are relatively suppressed since the gluon propagator is $\sim 1/M_{Z' t\bar{t}}^2$ as opposed to $1/M_{t\bar{t}}^2$ in the case of initial-state radiation. This also explains why the $q\bar{q}$ contribution dominates the gluon contribution at $M_{Z'} = 1$ TeV even though the relative luminosities change only by a factor of about 2; the dominant $q\bar{q}$ graphs tend to give small $M_{t\bar{t}}$, whereas requiring $M_{t\bar{t}} \sim m_H \sim 130$ GeV cuts out most of the gg contribution. The resulting background, assuming $M_{Z' t\bar{t}} = M_{Z'} \pm 5\%$ and $M_{t\bar{t}} = m_H \pm 15$ GeV, is shown as the dashed curve in Fig. 1 for $m_H = 100$ GeV and $m_t = 40$ GeV. We have used the structure functions of Eichten *et al.*³⁴ though very similar results are obtained using those of Duke and Owens³⁵ (set I) with $\Lambda = 0.2$ GeV. We have also incorporated a cut $|y| < 4$ on the rapidities of Z , t , and \bar{t} . We see that for these resolutions, the signal is well above the background, over almost the whole range of parameters considered even after allowing for the uncertainties in the $Z^0 H_L$ cross sections discussion in Sec. II. We note here that a larger $M_{Z'}$ yields better signal-to-background ratios since the background cross section increases very fast with decreasing $M_{Z' t\bar{t}}$ due to the rapid increase of gluon luminosity.

It is clear that the background crucially depends on the experimental resolution that can be attained on the measurement of $M_{Z' t\bar{t}}$ and $M_{t\bar{t}}$. To study the effect of these resolutions on the background, we show the $Z^0 t\bar{t}$ background cross section for different bin widths around m_H and $M_{Z'}$ in Table II. Here we have fixed $M_{Z'} = 500$ GeV and $m_H = 130$ GeV. We see that the cross sections scale almost perfectly with the size of the bins except for the largest (80–160 GeV) bin around m_H where the lower end of the bin is at the phase-space boundary for $m_t = 40$ GeV. In this bin the cross section is smaller than that obtained by naive scaling as may be expected.

TABLE II. The cross section in pb from gluon fusion and $q\bar{q}$ annihilation (in parentheses) for $pp \rightarrow Z^0 t\bar{t}$ at $\sqrt{s} = 40$ TeV, with $M_{Z' t\bar{t}}$ and $M_{t\bar{t}}$ in the bins around 500 and 130 GeV, respectively.

$M_{Z' t\bar{t}}$ (GeV)	490–510	480–520	450–550
$M_{t\bar{t}}$ (GeV)			
125–135	0.072 (0.013)	0.15 (0.025)	0.39 (0.065)
120–140	0.14 (0.025)	0.29 (0.050)	0.77 (0.13)
115–145	0.22 (0.038)	0.44 (0.076)	1.16 (0.19)
110–150	0.29 (0.050)	0.58 (0.10)	1.53 (0.26)
100–160	0.43 (0.075)	0.87 (0.15)	2.31 (0.38)
80–160	0.48 (0.099)	0.96 (0.20)	2.57 (0.51)

From Fig. 1, for $M_{Z'}=500$ GeV, we see that our estimate of the signal ranges from 0.5 pb to $\gtrsim 10$ pb, depending on the assumptions. We thus see that signal-to-background ratios exceeding unity are possible for a wide range of parameters, allowing for reasonable experimental resolutions on the measurement of $M_{Z'i\bar{i}}$ and $M_{i\bar{i}}$.

We have also considered the possibility of enhancing the signal relative to background by looking at various distributions. The transverse-momentum distribution of the signal Z^0 is shown as the solid line in Fig. 4(a). We have taken $M_{Z'}=500$ GeV and $m_H=130$ GeV, with the normalization of the signal being determined using $\beta=45^\circ$ in the model of Ref. 6 and $B(H_L \rightarrow i\bar{i})=100\%$. The corresponding normalization for other parameters can be read off from Fig. 1 or from Eqs. (2.2) and (2.3). The Jacobian peak at

$$p_{TZ} = \lambda^{1/2}(M_{Z'}^2, M_{Z'}^2, m_H^2) / 2M_{Z'}$$

corresponding to the two-body decay of $Z^{0'}$ is clearly evident. An accurate measurement of its position would enable us to determine the Higgs-boson mass. Also shown in the figure are the corresponding distributions for the background for two choices of mass resolution (dashed lines). The lower curve corresponds to $M_{i\bar{i}}=m_H \pm 10$ GeV, $M_{Z'i\bar{i}}=M_{Z'} \pm 10$ GeV while the higher curve corresponds to $M_{i\bar{i}}=m_H \pm 30$ GeV, $M_{Z'i\bar{i}}=M_{Z'} \pm 50$ GeV. We note that the Jacobian peak is smeared for the case of the latter (probably more realistic) choice of resolution so that by looking for $Z^0 i\bar{i}$ events in the vicinity of the Jacobian peak one can enhance the signal-to-background ratio by an additional factor of around 4.

The distribution of azimuthal opening angle ($\phi_{i\bar{i}}$) between t and \bar{t} is shown in Fig. 4(b) for both the signal and the background for the same parameters as in Fig. 4(a). We see that for the case of the poorer resolution the $\phi_{i\bar{i}}$ distribution of the background significantly differs from that of the signal. If this angle can be experimentally measured, a further enhancement of the signal relative to background may be possible. We mention here that for the case of a ± 10 GeV resolution on $M_{Z'i\bar{i}}$ and $M_{i\bar{i}}$ (lower curves in Fig. 4), the signal and background have more or less similar distributions so that additional enhancement factors are not possible. However, the background, in this case, is sufficiently small that this is of no consequence. We also note that we have also studied the distribution of θ_Z , the angle between the Z^0 and the beam, and also that of the minimum of the angle between the Z^0 and t or Z^0 and \bar{t} . Both these distributions are virtually identical for signal and background so that no additional enhancement of signal-to-background ratio is possible. We conclude that it would be possible at the SSC to identify an intermediate-mass Higgs boson produced via $Z^{0'} \rightarrow Z^0 + H_L$ decays by looking for the $i\bar{i}$ decays of H_L , assuming reasonable resolutions on the mass of the $Z^0 i\bar{i}$ and $i\bar{i}$ systems. We now turn to the possibility of identifying H_L via its rarer supersymmetric decays.

(b) *Supersymmetric decays*³⁶ of H_L . We have seen in Sec. III that as many as 50% of the Higgs bosons may

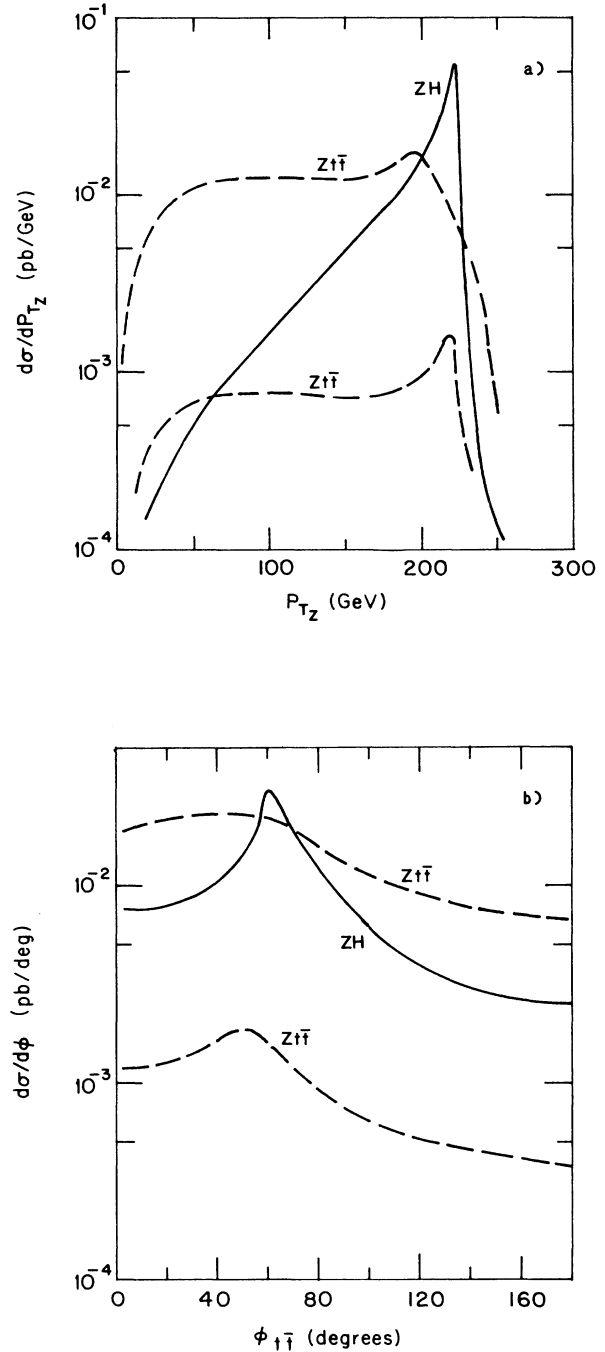


FIG. 4. (a) The transverse-momentum distribution $d\sigma/dp_{TZ}$ for the Z^0 boson and (b) the distribution of the azimuthal angle ($\phi_{i\bar{i}}$) between the t and \bar{t} quarks produced via $pp \rightarrow Z^{0'} \rightarrow Z^0 i\bar{i}$ (solid) and $pp \rightarrow gg, q\bar{q} \rightarrow Z^0 i\bar{i}$ (dashed curves). The solid curve is for the model of Ref. 6 with $M_{Z'}=500$ GeV, $m_H=130$ GeV, and $\beta=45^\circ$ assuming that the $Z^{0'}$ boson can only decay into standard fermions. The dashed curves have been obtained with $M_{i\bar{i}}=130 \pm 30$ GeV, $M_{Z'i\bar{i}}=500 \pm 50$ GeV (upper curve), and $M_{i\bar{i}}=130 \pm 10$ GeV, $M_{Z'i\bar{i}}=500 \pm 10$ GeV (lower curve). Again a rapidity cut $|y| < 4$ has been imposed on Z , t , and \bar{t} . The top-quark mass is taken to be 40 GeV.

decay via supersymmetric modes, $H_L \rightarrow \tilde{Z}_1 \tilde{Z}_1$, $H_L \rightarrow \tilde{Z}_1 \tilde{Z}_2$, $H_L \rightarrow \tilde{Z}_2 \tilde{Z}_2$, and $H_L \rightarrow \tilde{W} \tilde{W}$, even if we restrict ourselves to those parameters which yield $m_{\tilde{W}} \gtrsim 35$ GeV. We can classify the signals resulting from H_L decays according to the final states as follows. Since we assume \tilde{Z}_1 escapes detection, we have

$$H_L \rightarrow \tilde{Z}_1 + \tilde{Z}_1 \quad (\cancel{p}_T) \quad (5.1)$$

$$H_L \rightarrow \tilde{Z}_1 + \tilde{Z}_2 \rightarrow \tilde{Z}_1 + \tilde{l} \tilde{l} \tilde{Z}_1 \quad (\text{dilepton} + \cancel{p}_T) \quad (5.2a)$$

$$\rightarrow \tilde{Z}_1 + \nu \tilde{\nu} \tilde{Z}_1 \quad (\cancel{p}_T) \quad (5.2b)$$

$$\rightarrow \tilde{Z}_1 + q \bar{q} \tilde{Z}_1 \quad [\text{jet(s)} + \cancel{p}_T], \quad (5.2c)$$

$$H_L \rightarrow \tilde{Z}_2 + \tilde{Z}_2 \rightarrow \tilde{Z}_1 \tilde{l} \tilde{l} + \tilde{Z}_1 \tilde{l} \tilde{l} \quad (4 \text{ leptons} + \cancel{p}_T) \quad (5.3a)$$

$$\rightarrow \tilde{Z}_1 \tilde{l} \tilde{l} + \tilde{Z}_1 \nu \tilde{\nu} \quad (\text{dilepton} + \cancel{p}_T) \quad (5.3b)$$

$$\rightarrow \tilde{Z}_1 \nu \tilde{\nu} + \tilde{Z}_1 \nu \tilde{\nu} \quad (\cancel{p}_T) \quad (5.3c)$$

$$\rightarrow \tilde{Z}_1 q \bar{q} + \tilde{Z}_1 q \bar{q} \quad [\text{jet(s)} + (\cancel{p}_T)] \quad (5.3d)$$

$$\rightarrow \tilde{Z}_1 q \bar{q} + \tilde{Z}_1 \nu \tilde{\nu} \quad [\text{jet(s)} + (\cancel{p}_T)] \quad (5.3e)$$

$$\rightarrow \tilde{Z}_1 q \bar{q} + \tilde{Z}_1 \tilde{l} \tilde{l} \quad [\text{jet(s)} + \text{lepton(s)} + (\cancel{p}_T)], \quad (5.3f)$$

$$H_L \rightarrow \tilde{W} \tilde{W} \rightarrow \tilde{Z}_1 \tilde{l} \tilde{\nu} + \tilde{Z}_1 \tilde{l} \tilde{\nu} \quad (\text{dilepton} + \cancel{p}_T) \quad (5.4a)$$

$$\rightarrow \tilde{Z}_1 \tilde{l} \tilde{\nu} + \tilde{Z}_1 q \bar{q}' \quad (\text{lepton} + \text{jet(s)} + \cancel{p}_T) \quad (5.4b)$$

$$\rightarrow \tilde{Z}_1 q \bar{q}' + \tilde{Z}_1 q' \bar{q} \quad [\text{jet(s)} + \cancel{p}_T]. \quad (5.4c)$$

In addition we may also have the $\tilde{Z}_2 \rightarrow \tilde{W}$ events discussed in the last section so that we have

$$H_L \rightarrow \tilde{Z}_1 + \tilde{Z}_2 \rightarrow \tilde{Z}_1 + \tilde{W} q \bar{q}' \quad (5.5a)$$

$$\rightarrow \tilde{Z}_1 + \tilde{W} \tilde{l} \tilde{\nu} \quad (5.5b)$$

and a long list for \tilde{W} decays from $\tilde{Z}_2 \tilde{Z}_2$ events which we do not include for brevity. In Eqs. (5.1)–(5.5), we have not explicitly included the Z^0 boson which is present in all the events.

Here we concentrate on events that are essentially free of hadronic activity (except for QCD radiative corrections and multiple scattering) since these have smaller standard-model backgrounds. This reduces our classification of event topologies resulting from $Z^0 \rightarrow Z^0 + H_L$ decays to the following.

(A) $Z^0 + \cancel{p}_T$ events from (5.1), (5.2b), and (5.3c).

(B) $Z^0 + \text{dilepton} + \cancel{p}_T$ events from (5.2a), (5.3b), (5.4a), and (5.5b) if \tilde{W} decays leptonically.

(C) $Z^0 + n$ lepton + \cancel{p}_T events with $n \geq 3$ from (5.3a) and from \tilde{Z}_2 pairs events with one $\tilde{Z}_2 \rightarrow \tilde{l} \tilde{l} \tilde{Z}_1$ and the other $\tilde{Z}_2 \rightarrow \tilde{l} \tilde{\nu} \tilde{W}$, $\tilde{W} \rightarrow \tilde{l} \tilde{\nu} \tilde{Z}_1$. Such events are also possible if both \tilde{Z}_2 's decay into the $\tilde{l} \tilde{\nu} \tilde{W}$ mode. The $\tilde{Z}_2 \rightarrow \tilde{W}$ decays are interesting since they lead to the possibility $\tilde{Z}_2 \rightarrow e \mu + \cancel{p}_T$, though only in $\sim 2\%$ of the $\tilde{Z} \rightarrow \tilde{W}$ decays.

We remind the reader that we trigger on the leptonic decays of Z^0 so that the events are at least free from QCD backgrounds. We now consider the rates and backgrounds for each of the three classes of events, in turn.

(A) $Z^0 + \cancel{p}_T$ events. We see from Figs. 2 and 3 that the branching fraction for $H_L \rightarrow \tilde{Z}_1 \tilde{Z}_1$ production can exceed 20% if $\bar{\nu}/\nu > 0$. We also see from Table I that there is a substantial branching fraction for \tilde{Z}_2 to decay invisibly, particularly for $\bar{\nu}/\nu = 3$. In this case, about half or more of the $H_L \rightarrow \tilde{Z}_1 \tilde{Z}_2$ signal contributes to the invisible decay of H_L . Thus, at least for $\bar{\nu}/\nu > 0$, the invisible decays of the Higgs boson constitute 8–20% of its branching fraction. Here, as in the subsequent discussion, we assume that the supersymmetric decays of H_L are not kinematically suppressed. The p_T distribution of the Z^0 from these events, of course, has a Jacobian peak as before and is shown in Fig. 5 for $\beta = 45^\circ$ in the model of Ref. 6 assuming that H_L decays invisibly 10% of the time. The background dominantly comes from $Z^0 Z^0$ events with one of the Z^0 's decaying invisibly via $Z^0 \rightarrow \nu \bar{\nu}$, and the other leptonically. The p_T distribution of the visible Z^0 from the background is shown as the dashed curve in the figure. We see that for a Z^0 mass of 0.5 TeV, the Jacobian peak sticks well above the background, whereas for $M_{Z^0} = 300$ GeV it is just below the background. We emphasize again that the signal may be as much as a factor of 10 bigger due to a larger production cross section (see Fig. 1) and/or bigger branching fraction of H_L into the invisible mode. For the normalization shown in the figure (corresponding to about the middle of the band in Fig. 1), we may expect a signal cross section of ~ 0.01 pb for $M_{Z^0} = 0.5$ GeV after taking into account a 6% branching fraction for $Z^0 \rightarrow e \bar{e}$ or $\mu \bar{\mu}$. This corresponds to about 100 $Z^0 \rightarrow e^+ e^-$ or $\mu^+ \mu^- + \cancel{p}_T$ events per year at the SSC, assuming an annual integrated luminosity of 10^4 pb $^{-1}$. We remind the reader that a higher rate may be possible if $H_L \rightarrow \tilde{\nu} \tilde{\nu}$ de-

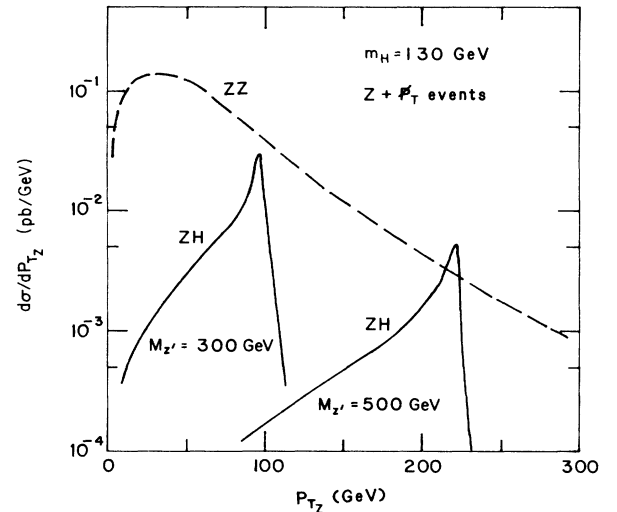


FIG. 5. Transverse-momentum distribution $d\sigma/dp_{TZ}$ for the Z^0 boson from $pp \rightarrow Z^0 \rightarrow Z^0 + H_L$ with H_L decaying invisibly (solid curves) and $pp \rightarrow q \bar{q} \rightarrow Z^0 Z^0$ with one of the Z^0 's decaying via $Z^0 \rightarrow \nu \bar{\nu}$ (dashed curve). The solid curves are for the model of Ref. 6 with $M_{Z^0} = 300$ and 500 GeV, respectively, assuming that invisible decays account for 10% of the total H_L decay width. The values of the other parameters are as in Fig. 4. The rapidities of the Z^0 bosons have been constrained to $|y| < 4$.

cays are kinematically accessible since a light scalar neutrino is expected to decay invisibly.²⁷ These events are all free from hadronic activity and should be observable over the standard-model background.

Before proceeding to discuss events of the (B) and (C) types, we note that $H_L \rightarrow \tilde{Z}_1 \tilde{Z}_2$, $\tilde{Z}_2 \tilde{Z}_2$, or $\tilde{W} \tilde{W}$ can also lead to quiet dilepton events if one of the \tilde{Z}_2 or both the \tilde{W} 's decay leptonically and the Z^0 produced in association with H_L decays via $Z^0 \rightarrow \nu \bar{\nu}$. In this case the dilepton mass gives a broad distribution bounded by $m_{\tilde{Z}_2} - m_{\tilde{Z}_1}$ for events from \tilde{Z}_2 decay. The decay $H_L \rightarrow \tilde{W} \tilde{W}$ gives a comparable number of dileptons for $\bar{\nu}/\nu > 0$. For these decays, however, it is not possible to enhance the signal via a Jacobian peak construction since both Z^0 and the escaping \tilde{Z}_1 contribute to \cancel{p}_T . The dominant background to these topologies comes from $W^+ W^-$ with both W 's decaying leptonically. We have not studied this background and so we will not discuss these events any further.

(B) $Z^0 + \text{dilepton events}$. As we have just seen, the case $\bar{\nu}/\nu > 0$ was characterized by the substantial invisible decay of H_L . The case $\bar{\nu}/\nu < 0$, as can be seen from Table I is characterized by the very substantial (20–30%) branching fraction of \tilde{Z}_2 into each family of charged leptons. This leads to the possibility of four-lepton + \cancel{p}_T events, with two of the leptons making up the Z^0 mass while the other leptons make a broad distribution in invariant mass. In addition, there would be a small number of events from the $\tilde{Z}_2 \rightarrow \tilde{W}$ decays (5.4a) and (5.5b), where at least one of the leptons would be rather soft. For $\bar{\nu}/\nu < 0$, H_L branching fractions into $\tilde{W} \tilde{W}$, $\tilde{Z}_2 \tilde{Z}_1$, and $\tilde{Z}_2 \tilde{Z}_2$ pairs are $\sim 8\text{--}20\%$, $1\text{--}2\%$, and $5\text{--}12\%$, respectively. Folding this with model-dependent branching fractions of $\sim 4\%$, $40\text{--}60\%$ and $10\text{--}20\%$ for the $\tilde{W} \tilde{W}$, $\tilde{Z}_1 \tilde{Z}_2$, and $\tilde{Z}_2 \tilde{Z}_2$ systems to decay into dileptons + \cancel{p}_T (see Table I), we find a rate of $20\text{--}70 \bar{l} l + (Z^0 \rightarrow l' \bar{l}')$ events per 10^4 pb^{-1} at the SSC, again assuming a $Z^0 H_L$ production cross section of $\sim 2 \text{ pb}$. We emphasize that these events are very clean and should stand out. Standard-model backgrounds to these come from $W^+ W^- Z^0$ production, with both W 's decaying leptonically. We have not estimated these in this paper. We note that events of the type (B) would also be present for $\bar{\nu}/\nu > 0$. In this case, the smallness of the branching fraction for $\tilde{Z}_2 \rightarrow \bar{l} l \tilde{Z}_1$ is compensated by the increase in that for $H_L \rightarrow \tilde{Z}_1 \tilde{Z}_2$. A comparable event rate may be expected.

(C) $Z^0 + n \text{ lepton events}$, $n \geq 3$. Major sources of these events are the decays (5.3a) and (5.5b). The contribution from $\tilde{Z}_2 \rightarrow \tilde{W}$ decays is small since it requires the leptonic decay of \tilde{Z}_2 as well as \tilde{W} (branching fraction $\sim 4\%$). The decays $H_L \rightarrow \tilde{Z}_2 \tilde{Z}_2$ have the largest branching fractions for $\bar{\nu}/\nu < 0$ for which the branching fraction is between $5\text{--}12\%$ when the decay is kinematically possible. For this sign of $\bar{\nu}/\nu$, the charged-leptonic branching fraction for \tilde{Z}_2 decay is $0.15\text{--}0.3$ per family. Again assuming a $Z^0 H_L$ production cross section of 2 pb , $10\text{--}50$ six charged-lepton events (lepton means e or μ) with two of the leptons making up Z^0 are expected annually at the SSC. For the other sign of $\bar{\nu}/\nu$, the rate of multilep-

ton events is small from all the sources considered.

In addition to the clean events discussed above, there will be a number of $Z^0 + \text{multijet} + \cancel{p}_T$ and $Z^0 + \text{multijet} + \text{lepton} + \cancel{p}_T$ events mostly coming from \tilde{W} decays. Here \tilde{W} may originate from $H_L \rightarrow \tilde{W} \tilde{W}$ or from $\tilde{Z}_2 \rightarrow \tilde{W}$ decays. Typical branching fractions for $H_L \rightarrow \tilde{W} \tilde{W}$ are $10\text{--}20\%$. Folding this with the \tilde{W} branching fraction shown in Table I, we find, assuming a 2-pb cross section for $Z^0 H_L$ production, that there are ~ 100 multijet + $(Z^0 \rightarrow \bar{l} l) + \cancel{p}_T$ events per 10^4 pb^{-1} at the SSC and about half as many jet(s) + lepton + $(Z^0 \rightarrow \bar{l} l) + \cancel{p}_T$ events from $\tilde{W} \tilde{W}$ decays of H_L . We emphasize that there are standard-model sources for these event topologies so that it would be difficult to isolate H_L events without a detailed background analysis.

In summary, we have seen that the supersymmetric decays of the Higgs boson lead to a number of very characteristic multilepton + \cancel{p}_T events which may be present if \tilde{W} and \tilde{Z}_2 are light enough to be produced in these decays. These events would be present in addition to the $Z^0 \bar{l} l$ events and would serve to corroborate the Higgs-boson signal. We also note that we have assumed in our analysis that the t quark is light enough to be produced via H_L decays. If this is not the case, the supersymmetric decays of H_L discussed in Sec. III become dominant unless they are kinematically inaccessible. It seems unlikely though that the decay $H_L \rightarrow \tilde{Z}_1 \tilde{Z}_1$ would be kinematically disallowed so that the large branching fraction for the invisible decay of the Higgs boson may well serve to provide a clear signature. Finally, we note that if m_H is large enough for it to decay into gauge-boson pairs (although this is not expected in the class of models considered), three-gauge-boson production with the mass of the three-particle system peaking at $M_{Z'}$ and of the two-particle system peaking at m_H may provide a clear signature.

VI. SUMMARY AND CONCLUDING REMARKS

In this paper we have studied promising new signals for the detection of the lightest Higgs boson (H_L) produced via the decay $Z^{0'} \rightarrow Z^0 H_L$ (Refs. 11 and 13) where $Z^{0'}$ is the extra neutral gauge boson that is expected to be present in the currently popular E_6 supergravity models. We have shown that if the mass of $Z^{0'}$ is less than about 0.6 TeV , in excess of $10^4\text{--}10^5$ $Z^0 H_L$ pairs would be expected to be produced annually at a 40-TeV pp collider such as the SSC, assuming an integrated luminosity of $10^4 \text{ pb}^{-1}/\text{yr}$. As discussed in Sec. I, H_L is expected to be relatively light¹² ($\lesssim 170 \text{ GeV}$ if E_6 breaks directly to a rank-5 group and $\lesssim 210 \text{ GeV}$ if we allow for an intermediate scale $\sim 10^{10} \text{ GeV}$), so that the decay $Z^{0'} \rightarrow Z^0 + H_L$ is unlikely to be kinematically suppressed, especially in view of the cosmological mass bound $M_{Z'} > 330\text{--}400 \text{ GeV}$ (Refs. 9 and 10) obtained from the successful predictions of nucleosynthesis.

This relatively small mass of H_L also implies that its decay into gauge-boson pairs is likely to be kinematically suppressed, so that the decay $H_L \rightarrow t \bar{t}$ will dominate unless the top-quark mass exceeds $m_H/2$. A Higgs boson lighter than $40\text{--}60 \text{ GeV}$ should be discovered at CERN

LEP I (Ref. 37) while LEP II should be able to probe Higgs-boson masses up to ~ 100 GeV (Ref. 38). In most of our analysis, we have, therefore, assumed that the Higgs-boson mass is large enough so that it can decay into $t\bar{t}$ pairs with $m_t = 40$ GeV but not into W^+W^- and Z^0Z^0 pairs. As is well known,³⁹ there is no clean signature for detecting such an intermediate-mass standard-model Higgs boson at the SSC, with the possible exception of the decay of a fourth-generation pseudoscalar quarkonium into a Z^0 -Higgs-boson pair.⁴⁰

In the E_6 models we are considering the $Z^{0'}$ resonance leads to a vastly enhanced rate for associated Z^0 -Higgs-boson production. In Sec. II we have discussed in detail the various theoretical uncertainties in the estimate of this cross section. Our results are shown in Fig. 1. We see that in spite of model uncertainties of a factor of about 20, more than 10^4 Z^0H_L pairs are expected annually at the SSC for a wide class of models and for $M_{Z'} \sim 0.5$ TeV. This large event rate allows us to trigger on the clean leptonic decay of the Z^0 in searching for the Higgs-boson signal. If H_L decays via $H_L \rightarrow t\bar{t}$, the signal is characterized by a $Z^0t\bar{t}$ final state with $M_{Zt\bar{t}} \sim M_{Z'}$ and $M_{t\bar{t}} \sim m_H$. Assuming a reasonable efficiency for top-quark identification and reasonable values of experimental resolutions on the measurement of $M_{Zt\bar{t}}$ and $M_{t\bar{t}}$ (see Table II) we have shown that a signal-to-background ratio substantially exceeding unity can be achieved for a wide range of parameters. For $m_H = 130$ GeV and $M_{Z'} \sim 0.5$ TeV, about 600–1500 $t\bar{t} + (Z^0 \rightarrow l^+l^-)$ signal events may be expected annually at the SSC if the H_L decays exclusively into $t\bar{t}$ pairs.

In Sec. III we have considered the possibility of supersymmetric decays of H_L . We have shown that if $M_{Z'} \gg M_Z$, H_L decays into the lightest chargino pair and into the two lightest neutralinos can be as large as 65% even assuming that $m_{\tilde{W}} > 35$ GeV. The exact branching fractions into the various modes depend sensitively on the model parameters and are summarized in Figs. 2 and 3.

We have studied the subsequent decays of \tilde{W} and \tilde{Z}_2 in Sec. IV. We find that \tilde{W} decays leptonically about one-third of the time almost independently of our assumptions. The decays of \tilde{Z}_2 , however, are much more model dependent; \tilde{Z}_2 may decay dominantly into charged leptons, invisibly into $\nu\bar{\nu}\tilde{Z}_1$, or via the $\tilde{Z}_2 \rightarrow \tilde{W}\bar{l}\nu$ and $\tilde{Z}_2 \rightarrow \tilde{W}u\bar{d}$ modes. The corresponding branching fractions are summarized in Table I. We see that the hadronic decays $\tilde{Z}_2 \rightarrow \tilde{Z}_1 q\bar{q}$ are relatively suppressed. This is because the scalar quark, in this class of models, is much heavier than the scalar neutrino and the scalar lepton. We note here that the branching fractions shown in the table are sensitive to our assumption that the scalar-fermion mass and the gaugino mass at the unification scale are about equal. If the ratio of

m_0 to $m_{1/2}$ is much smaller than one,^{6,29} \tilde{e}_L and $\tilde{\nu}_L$ can become quite light in the model of Ref. 6 because of the negative $\tilde{U}(1)$ D terms. In this case, the \tilde{Z}_2 decay patterns may be quite different. This is quite straightforward to incorporate.

The supersymmetric decays of H_L lead to additional interesting signatures for the process $Z^{0'} \rightarrow Z^0 + H_L$. The invisible decays of H_L produced in association with Z^0 (which is identified via its leptonic decay) lead to about 100 $Z^0 \rightarrow l^+l^-$ events per year with Z^0 recoiling against \cancel{p}_T at the SSC, if $M_{Z'} \sim 0.5$ TeV. The standard-model background comes from Z^0 -pair production with one of the Z^0 's decaying into charged leptons and the other into neutrinos. As seen from Fig. 5, the signal has a Jacobian peak which sticks out well over the background for $M_{Z'} = 0.5$ TeV and is just below the background for $M_{Z'} = 0.3$ TeV. In addition, the decays of H_L into $\tilde{W}\tilde{W}$, $\tilde{Z}_1\tilde{Z}_2$ and $\tilde{Z}_2\tilde{Z}_2$ pairs in conjunction with $Z^0 \rightarrow l^+l^-$ decays lead to about 20–70 characteristic four-lepton $+\cancel{p}_T$ events and about 10–50 spectacular six-lepton $+\cancel{p}_T$ events (only if $\bar{\nu}/\nu < 0$) that are essentially free of hadronic activity. We emphasize here that the supersymmetric decays of H_L may be important in searching for the Higgs boson via other processes.

To conclude, we have shown that the decay $Z^{0'} \rightarrow Z^0 + H_L$ leads to promising new ways of detecting the intermediate-mass Higgs boson at the SSC if the mass of $Z^{0'}$ is 300–700 GeV. In addition to the dominant $Z^0t\bar{t}$ signal, supersymmetric decays of the Higgs boson may also lead to clean $Z^0 + \cancel{p}_T$ and $Z^0 + \text{multilepton} + \cancel{p}_T$ signatures.

Note added in proof. After completion of this paper, it was recognized that the 12×12 neutral-fermion sector, the 4×4 charged-fermion sector, and the 9×9 neutral-Higgs-boson sector do not, in general, decouple as stated in Ref. 16 and the unpublished version of Ref. 17. Rather, there are two possible vacuum solutions, only one of which leads to the decoupling assumed in this paper. The results of this paper are thus valid in the class of models extensively discussed in the literature^{6,7,16,17,26} where the neutralino sector does break up as assumed. A further discussion of this point may be found in the published version of Ref. 17 and in Ref. 41.

ACKNOWLEDGMENTS

We thank S. Nandi for helpful conversations. This research was supported in part by the University of Wisconsin Research Committee with funds granted by the Wisconsin Alumni Research foundation, and in part by the U.S. Department of Energy under Contracts Nos. DE-AC02-76ER00881, DE-FG05-ER8540200, and W-31-109-ENG-38.

¹M. Green and J. H. Schwarz, Phys. Lett. **149B**, 117 (1984).

²P. Candelas, G. Horowitz, A. Strominger, and E. Witten, Nucl. Phys. **B258**, 46 (1985).

³E. Witten, Nucl. Phys. **B258**, 75 (1985).

⁴M. Dine, V. Kaplunovsky, M. Mangano, C. Nappi, and N. Seiberg, Nucl. Phys. **B259**, 519 (1985); J. Breit, B. Ovrut and G. Segrè, Phys. Lett. **158B**, 33 (1985); A. Sen, Phys. Rev. Lett. **55**, 33 (1985).

- ⁵V. Barger, N. Deshpande, and K. Whisnant, *Phys. Rev. Lett.* **56**, 30 (1986); S. M. Barr, *ibid.* **55**, 2778 (1985); E. Cohen, J. Ellis, K. Enqvist, and D. V. Nanopoulos, *Phys. Lett.* **165B**, 76 (1985); M. Drees, N. K. Falck, and M. Glück, *ibid.* **167B**, 187 (1986); L. S. Durkin and P. Langacker, *ibid.* **166B**, 436 (1986).
- ⁶J. Ellis, K. Enqvist, D. V. Nanopoulos, and F. Zwirner, *Nucl. Phys.* **B276**, 14 (1986).
- ⁷L. E. Ibañez and J. Mas, *Nucl. Phys.* **B286**, 107 (1987).
- ⁸Y. Hosotani, *Phys. Lett.* **129B**, 193 (1983).
- ⁹G. Steigman, K. A. Olive, D. N. Schramm, and M. S. Turner, *Phys. Lett.* **176B**, 33 (1986).
- ¹⁰J. Ellis, K. Enqvist, D. V. Nanopoulos, and S. Sarkar, *Phys. Lett.* **167B**, 452 (1986).
- ¹¹T. G. Rizzo, *Phys. Rev. D* **34**, 1438 (1986); S. Nandi, *Phys. Lett.* **181B**, 325 (1986).
- ¹²M. Drees, *Phys. Rev. D* **35**, 2910 (1987).
- ¹³J. F. Gunion, L. Roszkowski, and H. E. Haber, *Phys. Lett.* **189B**, 409 (1987).
- ¹⁴J. F. Gunion and Z. Kunszt, in *Proceedings of the 1986 Summer Study of the Design and Utilization of the Superconducting Super Collider*, Snowmass, Colorado, edited by R. Donaldson and J. Marx (to be published).
- ¹⁵S. Ellis, R. Kleiss, and W. J. Stirling, *Phys. Lett.* **163B**, 261 (1985).
- ¹⁶B. Campbell, J. Ellis, K. Enqvist, J. S. Hagelin, D. V. Nanopoulos, and K. Olive, *Phys. Lett.* **173B**, 270 (1986).
- ¹⁷J. Ellis, D. V. Nanopoulos, S. T. Petcov, and F. Zwirner, *Nucl. Phys.* **B283**, 93 (1987).
- ¹⁸H. E. Haber and M. Sher, *Phys. Rev. D* **35**, 2206 (1987).
- ¹⁹See Barger, Deshpande, and Whisnant (Ref. 5).
- ²⁰J. Ellis, L. Ibañez, and G. G. Ross, *Nucl. Phys.* **B221**, 29 (1983); P. Nath, R. Arnowitt, and A. H. Chamseddine, *Phys. Lett.* **129B**, 445 (1983); J. Ellis, J. M. Frere, J. S. Hagelin, G. L. Kane, and S. Petcov, *ibid.* **132B**, 436 (1983); B. Grinstein, J. Polchinski, and M. Wise, *ibid.* **130B**, 285 (1983); D. A. Dicus, S. Nandi, and X. Tata, *ibid.* **129B**, 451 (1983); S. Dawson, E. Eichten, and C. Quigg, *Phys. Rev. D* **31**, 1581 (1985); H. E. Haber and G. L. Kane, *Phys. Rep.* **117**, 75 (1985); R. M. Barnett and H. E. Haber, *Phys. Rev. D* **31**, 85 (1985); A. Bartl, H. Fraas, and W. Majerotto, *Z. Phys. C* **30**, 441 (1986); H. Komatsu and J. Kubo, *Nucl. Phys.* **B263**, 265 (1986); X. Tata and D. A. Dicus, *Phys. Rev. D* **35**, 2110 (1987).
- ²¹H. Baer, V. Barger, D. Karatas, and X. Tata, *Phys. Rev. D* **36**, 96 (1987).
- ²²This may also be deduced from the couplings in J. F. Gunion and H. E. Haber, *Nucl. Phys.* **B272**, 1 (1986); we have checked numerically that we get the same results using Eq. (3.1).
- ²³The supersymmetric Higgs-boson-mass term $2m_1$ of Ref. 21 is $\lambda n/\sqrt{2}$ here, while the angle α there is $(\pi/2 - \beta)$; furthermore, our \bar{H} is the H of Ref. 21.
- ²⁴H. Baer, K. Hagiwara, and X. Tata, *Phys. Rev. Lett.* **57**, 294 (1986); *Phys. Rev. D* **35**, 1598 (1987); A. H. Chamseddine, P. Nath, and R. Arnowitt, *Phys. Lett.* **174B**, 399 (1986); R. Arnowitt and P. Nath, *Phys. Rev. D* **35**, 1085 (1987). These analyses rely on the assumption of a light $\tilde{\gamma}$. Some effects of varying $m_{\tilde{\gamma}}$ have been studied by M. Glück, R. M. Godbole, and E. Reya, *Phys. Lett.* **186B**, 421 (1987). Although we restrict ourselves to $m_{\tilde{\gamma}} \gtrsim 35$ GeV, we note that allowing for smaller \tilde{W} masses only enhances the supersymmetric decays of H_L .
- ²⁵Under a simultaneous change of signs for ϵ and β , γ_L changes sign but γ_R is left unaltered. It is easy to see from the structure of the neutralino mass matrix that the relative sign between the two Higgs-fermion components of the eigenstates is also changed. It then follows from Eqs. (3.2) and (3.3) that the couplings S and X^{ij} are unaltered in magnitude and hence the partial widths for the supersymmetric decays of H_L are unchanged.
- ²⁶J. Ellis, K. Enqvist, D. V. Nanopoulos, and F. Zwirner, *Mod. Phys. Lett.* **A1**, 57 (1986); M. Drees, University of Wisconsin Report No. MAD/PH/328, 1987 (unpublished).
- ²⁷R. M. Barnett, H. E. Haber, and K. Lackner, *Phys. Lett.* **126B**, 64 (1983); J. S. Hagelin, G. L. Kane, and S. Raby, *Nucl. Phys.* **B242**, 638 (1984); L. Ibañez, *Phys. Lett.* **137B**, 160 (1984).
- ²⁸Drees (Ref. 26). In principle, the scalar masses could be smaller than given by Eq. (4.7) because of the presence of additional superpotential couplings. We do not investigate this possibility here.
- ²⁹J. Ellis, D. V. Nanopoulos, M. Quiros, and F. Zwirner, *Phys. Lett.* **180B**, 83 (1986); P. Binétruy, S. Dawson, I. Hinchliffe, and M. K. Gaillard, Berkeley Report No. LBL-22339 1986 (unpublished).
- ³⁰A. Font, F. Quevedo, and M. Quirós, *Phys. Lett.* **188B**, 75 (1987); S. Ferrara, A. Font, F. Quevedo, M. Quirós, and M. Villasante, *Nucl. Phys.* **B288**, 233 (1987).
- ³¹P. Nath, R. Arnowitt, and A. Chamseddine, Harvard Report No. HUTP 83/A077 (1983); Baer, Hagiwara, and Tata (Ref. 24).
- ³²R. Arnowitt (private communication).
- ³³M. Duncan and P. Langacker, *Nucl. Phys.* **B277**, 285 (1986); V. Barger, N. Deshpande, J. Rosner, and K. Whisnant, *Phys. Rev. D* **35**, 2893 (1986); V. Barger, N. G. Deshpande, and K. Whisnant, *ibid.* **35**, 1005 (1987); B. Adeva, F. Del Aguila, D. V. Nanopoulos, M. Quiros, and F. Zwirner, in *Proceedings of the 1986 Summer Study of the Design and Utilization of the Superconducting Super Collider*, Snowmass, Colorado (Ref. 14).
- ³⁴E. Eichten, I. Hinchliffe, K. Lane, and C. Quigg, *Rev. Mod. Phys.* **56**, 579 (1984); **58**, 1065(E) (1986).
- ³⁵D. W. Duke and J. F. Owens, *Phys. Rev. D* **30**, 49 (1984).
- ³⁶These have been discussed for the heavier neutral Higgs boson in minimal supergravity in J. F. Gunion and H. E. Haber, *Nucl. Phys.* **B228**, 449 (1986); and R. M. Barnett, J. A. Grifols, A. Mendez, J. F. Gunion, and J. Kalinowski, in *Proceedings of the 1986 Summer Study of the Design and Utilization of the Superconducting Super Collider*, Snowmass, Colorado (Ref. 14). In the given model, however, this Higgs boson is probably too heavy to be produced in Z^0 decays (see Refs. 18 and 12).
- ³⁷H. Baer *et al.*, in *Physics at LEP*, LEP Physics Jamboree, Geneva, Switzerland, 1985, edited by J. Ellis and R. Peccei (CERN Yellow Report No. 86-02, 1986), Vol. I, p. 297; D. Atwood, A. Contogouris, N. Mebarki, and H. Tanaka, *Phys. Rev. D* **34**, 2648 (1986).
- ³⁸G. Barbiellini *et al.*, in *Physics at LEP* (Ref. 37), Vol. II, p. 1.
- ³⁹J. F. Gunion, P. Kalyniak, M. Soldate, and P. Galison, *Phys. Rev. D* **34**, 101 (1986).
- ⁴⁰V. Barger *et al.*, *Phys. Rev. Lett.* **57**, 1672 (1986); *Phys. Rev. D* **35**, 3366 (1987).
- ⁴¹M. Drees and X. Tata, *Phys. Lett. B* (to be published).